Global Ocean Data Set of Marine Aerosol Properties

Patricia K. Quinn[1], Timothy S. Bates[2], Derek J. Coffman[1], James E. Johnson[2], Lucia M. Upchurch[2], and Hanna Best[2]

[1]NOAA Pacific Marine Environmental Laboratory, Seattle, WA, USA
[2]Cooperative Institute for Climate Ocean and Ecosystem Studies (CICOES), University of Washington, Seattle, WA, USA

Correspondence to: Patricia K. Quinn (patricia.k.quinn@noaa.gov)

Abstract. NOAA's Pacific Marine Environmental Laboratory (PMEL) has made measurements of aerosol chemical, microphysical, optical, and cloud nucleating properties onboard research cruises since 1991. The twenty-five cruises have covered all of the world's oceans -- the Pacific, Atlantic, Indian, Arctic, and Southern. The result is the most comprehensive, publicly available database of aerosol properties in the marine atmosphere to date. The database also contains gas-phase species (O_3, SO_2, Radon, and dimethylsulfide (DMS), seawater species (DMS, NH_4^+, NO_3^-, and chlorophyll-a), and meteorological parameters. Details of the cruises (locations, dates, and objectives), parameters measured, instrumentation used, and data availability are provided here. Also included are PMEL's high-level major findings and past usage of the data by others. The goal of this paper is to promote broader awareness of the database to the atmospheric aerosol *in situ* measurement, satellite, and modelling communities. Data are publicly available at NOAA's National Centers for Environmental Information (NCEI) data archive (https://www.ncei.noaa.gov/). Links to the Digital Object Identifiers (DOIs) for each cruise are provided herein.

Deleted: to date

Deleted:

1 Introduction

Aerosol particles influence Earth's radiation budget directly by scattering and absorbing incoming solar radiation and indirectly by acting as cloud condensation nuclei (CCN) and impacting cloud properties including reflectivity, lifetime, and spatial extent. The concentration and composition of aerosol particles vary both geographically and temporally, leading to a wide range of local and global climate impacts. Over oceans, aerosol particles have both continental and oceanic sources. Particles emitted from continental sources, including fossil fuel combustion, biomass burning, dust, and biogenic emissions, can be transported hundreds to thousands of kilometers over oceans either in the boundary layer or the free

troposphere (FT) (Clarke et al., 2013). Aerosol number and mass concentrations, chemical composition, and optical and cloud-nucleating properties are impacted by transport events and vary with distance from shore (Quinn et al., 2015). The ocean itself is a source of aerosol particles through wave-breaking at the surface and subsequent bubble bursting (De Leeuw et al., 2011). In addition, marine vessel emissions also contribute to the aerosol population over oceans, particularly in coastal regions and major shipping lanes (Corbett et al., 2007). Marine aerosol is defined here as particles in the atmosphere over oceans regardless of origin.

Observations of aerosol properties in the marine atmosphere are required to improve the accuracy of model simulations of their radiative effects. Satellite observations provide broad spatial and temporal coverage of the atmospheric aerosol burden over the world's oceans and reveal information about seasonally persistent transport from continents. Examples include the transport of African dust westward across the Atlantic every summer (Kaufman et al., 2005) and transport of Asian dust and pollution eastward across the Pacific during the spring (Logan et al., 2010). While satellite observations have the advantage of providing global coverage, *in situ* observations have the highest level of accuracy available to constrain radiative forcing and reduce uncertainties in forcing estimates (Li et al., 2022). As such, *in situ* measurements provide detailed information about the processes controlling variability in aerosol properties due to complex particle and gas phase precursor sources, transport pathways, and removal processes.

Cruises conducted since 1991 by PMEL cover all of the world's ocean providing the most comprehensive, publicly available global database to date of marine aerosol microphysical, chemical, optical, and cloud-nucleating properties. The data set is unique in that standardized methods and sampling protocols were employed including particle size cuts at a common relative humidity upstream of instrumentation and particle collection devices. This approach eliminates biases in the data and allows for direct comparison of measured regional properties between cruises. The global nature of the data set makes it well-posed to address current scientific priorities including reducing uncertainties in aerosol

radiative forcing and links between ocean biology climate. The details provided here describing the measurements in depth are intended to increase the usability of the data

The cruises were process oriented geared toward understanding the effects of formation, emission, atmospheric transformation and removal on aerosol properties. Some of the cruises were conducted during the time of the year when a targeted plume was expected to be most pronounced. For those cruises, the range of reported values most likely is skewed toward higher values that are typical of seasonally maximum plumes. In addition, reported variability in the data are based on a snapshot during the short-lived campaigns. Objectives are described and references are cited to provide context for each cruise.

This paper describes the measurements in detail, the data that are available for each cruise, PMEL's major findings, and data usage by others. The goal is to provide information about data availability and to advance the widespread use of the data to the atmospheric aerosol *in situ* measurement, satellite, and modelling communities. Sect. 2 describes the cruises and Sect. 3 describes the methods. PMEL's major findings are summarized in Sect. 4., data usage by others in Sect. 5, and a brief summary in Sect. 6. Data availability is described in Sect. 7.

2 Global Ocean Cruises

Ship tracks of PMEL's cruises between 1991 and 2020 are shown in Figure 1. A list of the cruises with start and stop dates, departure and arrival ports, location, and relevant references is provided in Table 1. A complete list of instrumentation on each cruise is presented in Section 3. Each cruise is briefly described in the following paragraphs.

The Pacific Stratus Sulfur Investigation, PSI-91 is the first cruise reported here. It took place in spring of 1991 in the eastern North Pacific off the coast of Washington state with the NOAA *R/V Discoverer* leaving from Seattle, WA in mid-April and returning in early May. Measurements focused on the role of

Formatted: Font: 12 pt, Not Bold

Deleted: Data were collected using standardized methods and sampling protocols to eliminate biases in the data and to allow for direct comparison between cruises.

DMS oxidation products in new particle production versus particle growth (Quinn et al., 1993; Covert et al., 1992) and the seawater sulfur cycle (Bates et al., 1994).

The Marine Aerosol and Gas Exchange cruise (MAGE92) took place in the tropical Pacific in 1992 with the USC *R/V John Vickers* leaving from Los Angeles, CA in mid-February, transiting to Nuka Hiva in the Marquesas Islands, and then returning to Los Angeles in late March. Similar to PSI-91, the goals of MAGE92 were to assess the seawater sulfur cycle and processes controlling the atmospheric aerosol particle number size distribution in the marine boundary layer (MBL) (Covert et al., 1996). In addition, instrumentation was augmented to include an integrating nephelometer to measure the aerosol light scattering coefficient at 550 nm (Charlson et al., 1967). The measurements were used to assess variability in aerosol chemical, microphysical, and optical properties relevant to direct radiative forcing (Quinn et al., 1995).

Figure 1. Cruise tracks for PMEL cruises between 1991 and 2020.

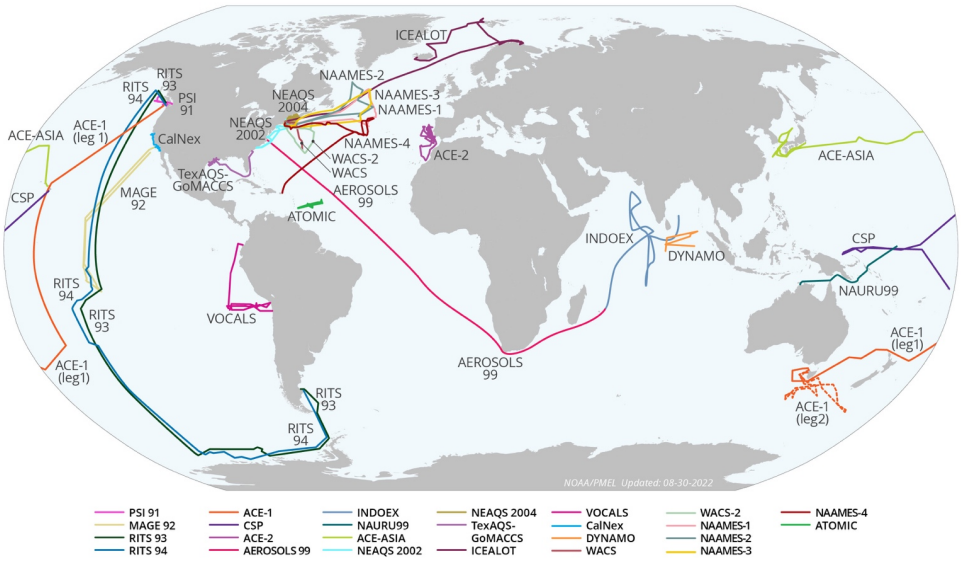

The Radiatively Important Trace Species (RITS) cruises, RITS93 and RITS94, took place between March and May 1993 and November 1993 and January 1994, respectively. During RITS93, the NOAA *R/V Surveyor* went from Palmer Station, Antarctica to the Gulf of Alaska while RITS94 went in the opposite direction. These cruises extended the measurements made during MAGE92 to the central Pacific between 55°N and 70°S (Quinn et al., 1996; Covert et al., 1996; Anderson et al., 1996).

In 1995, a series of Aerosol Characterization Experiments (ACE) was initiated under the auspices of the International Global Atmospheric Chemistry (IGAC) Project. The overall goal of ACE was to quantify the chemical and physical processes controlling the properties and evolution of aerosol particles relevant to radiative forcing and climate. Each experiment was multi-platform (research ships, aircraft, and ground stations) with international participation. The first Aerosol Characterization Experiment (ACE-1) took place in the Southern Ocean to target aerosol in a remote, minimally polluted marine atmosphere as a

reference for future experiments (Bates et al., 1998a). PMEL conducted measurements onboard the NOAA *R/V Discoverer* during Leg 1 from Seattle, WA, USA to Hobart, Australia and then Leg 2 in the Southern Ocean in and out of Hobart, Australia. ACE-1 extended earlier Pacific measurements to the Southern Ocean and augmented the characterization of optical properties through the addition of a single wavelength (550 nm) Particle Soot Absorption Photometer (PSAP) (Quinn et al., 1998b).

Subsequent ACEs were conducted downwind of continents to characterize changes in aerosol properties with advection over the ocean. ACE-2 was conducted in June and July of 1997 over the sub-tropical northeast Atlantic to characterize pollution and dust aerosol as it was advected from Europe and Africa and mixed into the marine atmosphere (Raes et al., 2000). PMEL made measurements onboard the Institute of Biology of the Southern Seas (IBSS) *R/V Professor Vodyanitskiy* leaving from and returning to Lisbon, Portugal. Background marine, anthropogenic, and dust aerosol were encountered (Bates et al., 2000). Instrumentation was unchanged from that of previous cruises.

The third experiment in the series was the Indian Ocean Experiment (INDOEX) which targeted the Indo-Asian haze during the Northern Hemisphere dry monsoon as it was advected over the Indian Ocean (Ramanathan et al., 2001). PMEL participated onboard the NOAA *R/V Ronald H. Brown* in a leg which brought the ship from Norfolk, VA to Mauritius during January and February of 1999. This leg was named AEROSOLS99. The second leg, officially INDOEX, took the ship from Mauritius northeast throughout the South Atlantic and Indian Oceans and ended in the Maldives during February and March of 1999. During both legs, marine background, anthropogenic, dust, and biomass burning aerosol were measured (Quinn et al., 2001). Trace element concentrations able to identify and quantify dust were added to the PMEL instrument payload for AEROSOLS99 and INDOEX.

Table 1. PMEL's cruises between 1991 and 2020 with start and stop dates, departure and arrival ports, ocean, and relevant references.

	Dates		Ports		Ocean(s)	References
	Start	Stop	Departure	Arrival		
PSI-91[a]	4/15/1991	5/1/1991	Seattle, WA, USA	Seattle, WA, USA	North Pacific (coastal Washington)	Covert et al. (1992); Quinn et al. (1993)

MAGE92[b]	2/21/1992	3/25/1992	Los Angeles, CA, USA	Nuka Hiva, Marquesas Islands	Tropical Pacific	Quinn et al. (1995)
RITS93[c]	3/20/1993	5/7/1993	Punta Arenas, Chile	Seattle, WA, USA	South and Tropical Pacific	Covert et al. (1996)
RITS94[d]	11/20/1993	1/7/1994	Seattle, WA, USA	Punta Arenas, Chile	North and Tropical Pacific	Covert et al. (1996)
ACE-1[e] Leg 1	10/12/1995	11/9/1995	Seattle, WA, USA	Hobart, Australia	Pacific	Bates et al. (1998a)
ACE-1[e] Leg 2	11/15/1995	12/13/1995	Hobart, Australia	Hobart, Australia	Southern Ocean	Bates et al. (1998a)
CSP[f]	3/12/1996	4/13/1996	Pago Pago, American Samoa	Honolulu, HI, USA	Tropical Pacific	Post et al. (1997)
ACE-2[g]	6/18/1997	7/24/1997	Lisbon, Portugal	Lisbon, Portugal	Northeast Atlantic	Raes et al. (2000)
AEROSOLS99	1/14/1999	2/8/1999	Norfolk, VA, USA	Cape Town, South Africa	Atlantic	Bates et al. (2001)
INDOEX[h]	2/22/1999	3/30/1999	Mauritius	Male, Maldives	South Atlantic and Indian	Ramanathan et al. (2001)
NAURU99[j]	6/15/1999	7/19/1999	Darwin, Australia	Kwajalein, Marshall Islands	Tropical Pacific	Post et al. (2000)
ACE-Asia[j]	3/15/2001	4/20/2001	Honolulu, HI, USA	Yokosuka, Japan	Western Pacific	Bates et al. (2004); Huebert et al. (2003)
NEAQS 2002[k]	7/12/2002	8/11/2002	Charleston, SC, USA	Charleston, SC, USA	Gulf of Maine, Atlantic Ocean	Bates et al. (2005)
NEAQS 2004[l]	7/5/2004	8/12/2004	Portsmouth, NH, USA	Portsmouth, NH, USA	Gulf of Maine, Atlantic Ocean	Fehsenfeld et al. (2006)
TexAQS-GoMACCS[m]	7/27/2006	9/11/2006	Charleston, SC, USA	Galveston, TX, USA	Gulf of Mexico	Parrish et al. (2009); Bates et al. (2008)
ICEALOT[n]	3/19/2008	4/24/2008	Woods Hole, MA, USA	Reykjavik, Iceland	North Atlantic, Arctic Ocean	Quinn et al. (2017); Russell et al. (2010)
VOCALS[o]	10/13/2008	12/2/2008	Panama City, Panama	Arica, Chile	Tropical Pacific	Hawkins et al. (2010); Wood et al. (2011)
CalNex[p]	5/14/2010	6/8/2010	San Diego, CA, USA	San Francisco, CA, USA	California Coast	Ryerson et al. (2013); Bates et al. (2012)
DYNAMO[q]	9/29/2011	12/8/2011	Phuket, Thailand	Phuket, Thailand	Indian Ocean	Dewitt et al. (2013)
WACS[r]	8/19/2012	8/27/2012	Boston, MA, USA	St. George's, Bermuda	North Atlantic	Quinn et al. (2014); Keene et al. (2017)
WACS2[s]	5/20/2014	6/5/2014	Woods Hole, MA, USA	Woods Hole, MA, USA	North Atlantic	Aller et al. (2017)
NAAMES1[t]	11/6/2015	12/1/2015	Woods Hole, MA, USA	Woods Hole, MA, USA	North Atlantic	Quinn et al. (2019); Quinn et al. (2017); Behrenfeld et al. (2019)

NAAMES2[t]	5/11/2016	6/5/2016	Woods Hole, MA, USA	Woods Hole, MA, USA	North Atlantic	Quinn et al. (2019); Quinn et al. (2017); Behrenfeld et al. (2019)
NAAMES3[t]	8/30/2017	9/24/2017	Woods Hole, MA, USA	Woods Hole, MA, USA	North Atlantic	Quinn et al. (2019); Quinn et al. (2017); Behrenfeld et al. (2019)
NAAMES4[t]	3/20/2018	4/13/2018	San Juan, Puerto Rico	Woods Hole, MA, USA	Tropical and North Atlantic	Quinn et al. (2019) Behrenfeld et al. (2019)
ATOMIC[u]	1/7/2020	2/13/2020	Bridgetown, Barbados	Bridgetown, Barbados	Tropical Atlantic	Quinn et al. (2021)

[a]Pacific Stratus Sulfur Investigation 1991
[b]Marine Aerosol and Gas Exchange 1992
[c]Radiatively Important Trace Species 1993
[d]Radiatively Important Trace Species 1994
[e]Aerosol Characterization Experiment-1 (https://data.eol.ucar.edu/project/ACE-1)
[f]Combined Sensor Program (https://psl.noaa.gov/psd3/air-sea/csp/)
[g]Aerosol Characterization Experiment-2
[h]Indian Ocean Experiment (http://www-indoex.ucsd.edu/index.html)
[i]https://psl.noaa.gov/psd3/air-sea/nauru99/
[j]Aerosol Characterization Experiment-Asia (https://www.eol.ucar.edu/field_projects/ace-asia)
[k]New England Air Quality Study 2002 (https://csl.noaa.gov/projects/neaqs/)
[l]New England Air Quality Study and International Consortium for Atmospheric Research on Transport and Transformation 2004 (https://csl.noaa.gov/projects/icartt/)
[m]Texas Air Quality Study/Gulf of Mexico Atmospheric Composition and Climate Study (https://csl.noaa.gov/projects/2006/)
[n]International Chemistry Experiment in the Arctic Lower Troposphere
[o]VAMOS Ocean-Cloud-Atmosphere-Land Study (https://www.eol.ucar.edu/field_projects/vocals)
[p]California Research at the Nexus of Air Quality and Climate Change (https://csl.noaa.gov/projects/calnex/)
[q]Dynamics of the Madden-Julian Oscillation (https://www.eol.ucar.edu/field_projects/dynamo)
[r]Western Atlantic Climate Study 2012
[s]Western Atlantic Climate Study 2014 (https://saga.pmel.noaa.gov/field_WACS2)
[t]The North Atlantic Aerosols and Marine Ecosystem Study-1 (https://science.larc.nasa.gov/NAAMES/)
[u]Atlantic Tradewind Ocean-Atmosphere Mesoscale Interaction Campaign (https://psl.noaa.gov/atomic/)

ACE-Asia, the fourth and final of the ACEs, was conducted in March through May of 2001 downwind of eastern Asia to target seasonal outbreaks of Asian dust associated with frontal systems moving to the east through dust-producing regions (Huebert et al., 2003). PMEL sampled onboard the NOAA *R/V Ronald H. Brown* from mid-March to mid-April in 2001 as the ship transited from Honolulu, HI to the western Pacific and then spent time east of Japan and in the Sea of Japan. Between Honolulu and 2,000 mile east of Japan, marine air minimally impacted by continental emissions was sampled. West onward from that

point, air masses heavily influenced by Asian emissions were sampled (Bates et al., 2004). Measurements of organic carbon (OC) and elemental carbon (EC) were added to the instrument payload for ACE-Asia.

During the ACE years, PMEL participated in two other cruises, the Combined Sensor Program (CSP) in March and April 1996 and NAURU99 in June and July of 1999. CSP took place in the central and tropical western Pacific with the NOAA *R/V Discoverer* leaving from Pago Pago, American Samoa in mid-March and arriving in Honolulu, HI in mid-April. The overarching goal of CSP was to better understand relationships between atmospheric and oceanic variables that affect radiative balance, including aerosol particles (Post et al., 1997). NAURU99 took place onboard the NOAA *R/V Ronald H. Brown* in the southwestern Pacific in the vicinity of Nauru Island in Papua New Guinea. NAURU99 had similar scientific goals as CSP and, in addition, was conducted to assess how representative measurements made on the islands of Nauru and Manus were of the surrounding ocean (Post et al., 2000). The ship left Darwin, Australia in mid-June and arrived in Kwajalein in the Marshall Islands in mid-July.

In 2002, a series of air quality and climate field campaigns was initiated by NOAA with other agency and academic partners. These campaigns were designed to determine the atmospheric processes that control the production and distribution of air pollutants that impact air quality and climate in and downwind of several U.S. regions. These campaigns involved, to varying degrees, a combination of shipboard, aircraft, and ground-based measurements. The New England Air Quality Study in 2002 (NEAQS 2002) targeted factors controlling air quality in New England with measurements at a network of ground stations and a ship (Bates et al., 2005). The NOAA *R/V Ronald H. Brown* departed Charleston, SC in mid-July 2002 and transited northeast up the coast to New York City, Boston, and Acadia National Park in Maine. The ship returned to Charleston in mid-August 2002.

Deleted: 2

A second NEAQS in 2004 (NEAQS 2004) was conducted in conjunction with the joint North American and European International Consortium for Atmospheric Research on Transport and Transformation (ICARTT). The focus was on emissions from North America and their chemical transformations and removal during transport over the North Atlantic (Fehsenfeld et al., 2006). The NOAA *R/V Ronald H.*

Brown left Portsmouth, NH in early July, made several transits along the coasts of Massachusetts, New Hampshire, and Maine, and across the Gulf of Maine toward Nova Scotia (Quinn et al., 2006). A Quadruple Aerosol Mass Spectrometer (Q-AMS) (Jayne et al., 2000) was added to the PMEL instrument payload for the measurement of nonrefractory (NR) species where NR refers to chemical components that vaporize (< 5 sec) at the vaporizer temperature of ~550°C.

The next in the series of Air Quality – Climate cruises was the Texas Air Quality – Gulf of Mexico Atmospheric Composition and Climate Study (TexAQS/GoMACCS) between July and September in 2006. The goal was to assess the factors that control the formation and transport of air pollutants along the Gulf Coast of south eastern Texas and the impact the resulting species have on the radiative forcing of climate regionally and globally (Parrish et al., 2009). The NOAA *R/V Ronald H. Brown* left Charleston, SC at the end of July, headed south along the coast of Florida, transited across the Gulf of Mexico, and spent several weeks along the coast of Texas including in the Houston Ship Channel (Bates et al., 2008). The cruise ended mid-September in Galveston, TX. Measurements of the relative humidity dependence of light scattering and cloud condensation nuclei (CCN) concentrations were added to the existing PMEL instrument payload.

The final Air Quality – Climate field campaign was the 2010 California Research at the Nexus of Air Quality and Climate Change (CalNex) study. An emphasis was put on issues that are simultaneously relevant to both air pollution and climate including emission inventories, atmospheric transport and dispersion, atmospheric processing, and aerosol direct and indirect radiative effects (Ryerson et al., 2013). The Woods Hole Oceanographic Institution (WHOI) *R/V Atlantis* left from San Diego, CA in mid-May 2020, transited northward up the coast of California with incursions into the Ports of Los Angeles, Long Beach, San Francisco, and Oakland, and a trip up the Sacramento River (Bates et al., 2012).

In between TexAQS-GoMACCS and CalNex, PMEL participated in two other cruises. The International Chemistry Experiment in the Arctic Lower Troposphere (ICEALOT) took place as part of the 2008 International Polar Year (Russell et al., 2010). The focus was on the sources, transport, and climate impact

of anthropogenic aerosol and gas phase species in an ice-free region of the Arctic. The WHOI *R/V Knorr* left Woods Hole, MA mid-March, transited across the North Atlantic to the coast of Norway, then northwest to Svalbard, and southwest to Reykjavik, Iceland where the cruise concluded at the end of April.

The VAMOS Ocean-Cloud-Atmosphere-Land Study Regional Experiment (VOCALS), where VAMOS stands for Variability of the American Monsoon Systems, took place in October and November of 2008. VOCALs focused on assessing links between aerosols, clouds and precipitation and their impacts on marine stratocumulus radiative properties and couplings between the upper ocean and lower atmosphere (Wood et al., 2011). The NOAA *R/V Ronald H. Brown* left Panama City, Panama in mid-October, conducted several transits in the vicinity of 20°S from the coast to 85°W, and ended the cruise in Arica, Chile at the beginning of December (Hawkins et al., 2010).

DYNAMO, the Dynamics of the Madden-Julian Oscillation (MJO) field campaign was conducted to collect *in situ* observations to advance our understanding of MJO initiation processes and to improve MJO prediction (Yoneyama et al., 2013). PMEL's research focused on the effect of MJO-associated convection anomalies on aerosols in the marine boundary layer (Dewitt et al., 2013). The Scripps Institution of Oceanography *R/V Roger Revelle* left Phuket, Thailand at the end of September 2011 and transited to the vicinity of 0.1°N and 80.5°E where it was stationed for most of the experiment. The ship returned to Phuket on December 8.

Between 2012 and 2018, PMEL participated in a series of cruises to investigate the impacts of marine ecosystems on primary sea spray aerosol (SSA) and its cloud-nucleating properties. During each of these cruises a portion of the time was spent generating and sampling nascent primary SSA with Sea Sweep (Bates et al., 2012). The Sea Sweep data are available in the referenced data sets for WACS, WACS-2, and all four NAAMES cruises. These data are not discussed further since the emphasis here is on ambient aerosol. Data from the ambient atmospheric marine aerosol that was sampled when Sea Sweep was not in use are discussed here. The first Western Atlantic Climate Study (WACS) took place in 2012 and

focused on the high-chlorophyll, biologically productive region of Georges Bank off the coast of Cape Cod and the low-chlorophyll, oligotrophic Sargasso Sea (Quinn et al., 2014; Kawamura et al., 2017). The NOAA *R/V Ronald H. Brown* left Boston, MA in mid-August, spent time at the high- and low-chlorophyll stations, and arrived at St. George's Bermuda at the end of August.

The second WACS (WACS2) took place in 2014. The WHOI *R/V Knorr* left Woods Hole, MA in mid-May, went east to 60°W and south to 33°S stopping for stations at a range of low to high biologically productive surface seawater. Atmospheric sampling took place between stations. The ship arrived back in Woods Hole in the beginning of June (Aller et al., 2017).

PMEL participated in the NASA sponsored North Atlantic Aerosols and Marine Ecosystems Study (NAAMES), a series of field campaigns conducted to assess the seasonal impact of the western subarctic North Atlantic phytoplankton bloom on aerosols and clouds (Behrenfeld et al., 2019). Four cruises, onboard the WHOI *R/V Atlantis*, took place between November 2015 and April 2018, with each cruise targeting specific seasonal phases of the annual plankton cycle (Quinn et al., 2019). The general cruise track included a transit from Woods Hole, MA to 40°N and 40°W, a northward transit with several stations to 55°N across a range of stages in each plankton seasonal cycle, followed by a return to Woods Hole. The exception was NAAMES-4, which left from San Juan, Puerto Rico and ended in Woods Hole. In seasonal but not chronological order, NAAMES-1 took place in November 2015 targeting the initiation of the phytoplankton blooming phase, NAAMES-4 in March and April 2018 targeting the accumulation phase, NAAMES-2 in May and June targeting the bloom climax, and NAAMES-3 in September 2017 targeting the declining phase of the bloom. To accommodate Sea Sweep sampling, atmospheric sampling of trace elements, NR chemical species, and total aerosol mass was not conducted during any of the NAAMES cruises.

The final cruise in the global data set to date is the Atlantic Tradewind Ocean-Atmosphere Mesoscale Interaction Campaign (ATOMIC) which took place in the tropical North Atlantic east of Barbados in early 2020 (Stevens et al., 2021). The NOAA *R/V Ronald H. Brown* left Bridgetown, Barbados in early

January and spent time between Barbados and the Northwest Tropical Atlantic Station (NTAS) buoy 500 nm to the northeast to gather information on shallow atmospheric convection, the effects of aerosols and clouds on the ocean surface energy budget, and mesoscale oceanic processes (Quinn et al., 2022). Measurements of trace element and total aerosol mass concentrations were reinstated for ATOMIC but concentrations of NR chemical species were not.

3. Methods

Sampling methods evolved between 1991 and 2020 as the number of parameters to be measured increased and the technical capabilities of instrumentation improved. In addition, instruments were added or removed from the PMEL payload depending on the goals of each cruise. Instrumentation and its evolution are described in detail below including the sampling inlet and methods for the measurement of aerosol microphysical, chemical, optical, and cloud-nucleating properties. In addition, measurement methods of gas phase species and surface seawater properties are provided. Parameters measured during each cruise are listed in Table 2 (aerosol microphysical and cloud-nucleating), Table 3 (aerosol chemical composition), Table 4 (aerosol optical), and Table 5 (gas phase and seawater species).

For all cruises, instrumentation was housed in one or more 8 ft (2.44 m) tall shipping container(s) outfitted with power, air conditioning, and, in some cases, water. Unistrut was installed on inside walls for the securing of instrument racks, drawers, shelves, etc. A railing surrounding the sampling inlet was installed on the roof of the container for mounting of meteorological and other sensors.

3.1. Aerosol sampling inlet

For all cruises, an aerosol sampling mast was mounted on top of an 8 ft (2.44 m) tall shipping container converted to a laboratory as described above. Diagrams of the sampling inlet and connections to instrumentation are shown in Figure 2. Schematics for all parts of the sampling inlet can be found at https://www.pmel.noaa.gov/acg/gallery/aerosol-sampling-inlet-schematics. The container was mounted

Deleted: and

Deleted: a

as far forward of the ship's stack as possible to minimize contamination. To maintain nominally isokinetic flow and minimize the loss of supermicron particles, the inlet at the top of the mast was rotated into the relative wind first manually (PSI-91 to NAURU-99) and then automatically under computer control (ACE Asia through ATOMIC). The mast angle was recorded for post-cruise data analysis. Air entered the inlet through a 5 cm diameter hole, passed through an expansion cone, and then into the 20 cm diameter sampling mast. The flow through the mast was 1 m^3 min^{-1}. Individual 1.9 cm diameter stainless steel tubes extended into the base of the mast. These were connected to the various aerosol instruments in the laboratory container directly below the mast with carbon-embedded conductive tubing to prevent the loss of particles through static charging. Sampling of organics was added to the PMEL payload for ACE-Asia. Stainless steel tubing was added for the connections between the aerosol inlet and the instruments and impactors sampling for organic components.

During the initial cruise reported here, PSI-91, sample air from the mast was not conditioned, i.e., heated to control RH. Instead, aerosol was sampled at ambient RH (75 ± 9%) although all CPCs (Condensation Particle Counters) had diffusion dryers upstream to reduce the RH of the sample air to less than 30%. Aerosol microphysical properties were measured continuously with periods of contamination, calibration, and downtime removed from the final data set. To avoid contamination by the ship's stack, samples for chemical analysis were collected only when the particle number concentration measured at the top of the mast was less than 1000 cm^{-3}, the relative wind speed was greater than 3 m s^{-1}, and the relative wind direction was forward of the ship's beam (± 90°). This approach was employed during all cruises although the particle number concentration and relative wind speed and direction limits were varied depending on conditions.

Deleted: .

After PSI-91, the last 1.5 m of the inlet were heated to establish a low reference relative humidity. Heating allows for constant instrumental size segregation in spite of variations in ambient RH and results in measurements of aerosol chemical, microphysical, and optical properties that are directly comparable. During MAGE 92, RITS 93, RITS 94, and ACE-1, sample air was heated above ambient temperatures to reach an RH of < 25%. The target RH for the sample air was increased to 55 to 60% for ACE-2 and

following cruises because it is above the efflorescence humidity of most aerosol components and component mixtures (Carrico et al., 2003), which reduces particle bounce in impactors and simplifies thermodynamic equilibrium calculations of particle density and refractive index. There are a few exceptions to the target RH of 55 to 60%. The cold Arctic air temperatures during ICEALOT and the higher latitude portions of the NAAMES cruises made it difficult to obtain that RH. Instead, the aerosol was sampled at less than 25% RH during those conditions.

After RITS94 and before ACE-1, a temperature-controlled box was installed at the base of the sampling mast (Figure 2b and c). The box was heated above ambient temperatures to reduce cooling and condensation in sampling lines in the air-conditioned laboratory container and to maintain a uniform RH of the sampled air. Instrumental RH for the particle sizing systems is listed in Table 2.

The transmission efficiency of particles through the mast as a function of size was characterized after INDOEX in the Kirsten Wind Tunnel at the University of Washington (Bates et al., 2002). The Kirsten Wind Tunnel is a subsonic, closed circuit, double return wind tunnel. The mast was mounted under the wind tunnel with the rotatable cone on top extending into the test section of the tunnel. Two sets of propellers moved air through the test section at speeds of 7 to 20 m sec^{-1}. Aerosol particles were generated from a 10% polyethylene glycol solution (PEG-400 molecular weight mixed in distilled water) using a pressurized tank and spray nozzle downwind of the mast. Aerosol size distributions were measured from 0.56 to 14 µm using Aerodynamic Particle Sizers (APS 3320, TSI, St. Paul, MN). Larger particle sizes were the focus of these tests as comparisons of total particle number concentration during ACE-1 found agreement within ~ 20% of the NCAR C-130 airplane and ground stations. The aerosol generator was

Figure 2. Shown are schematics of the aerosol sampling inlet (left) and a flow chart indicating the flow of sample air from the inlet to the instrumentation (right). This flow chart depicts the maximum number of instruments deployed. Green represents the van the inlet is mounted on, orange represents the temperature controlled box at the base of the inlet, and blue represents the van next door housing additional real time instruments.

Deleted: *a)*

Deleted: *the aerosol sampling mast mounted on top of a laboratory container onboard the R/V Ronald H. Brown during ATOMIC in 2020, b) the temperature-controlled box housing sizing instruments and impactors at the base of the mast in the laboratory container, and c) tubing connecting the sampling mast to sizing instrumentation (left) and impactors (right).*

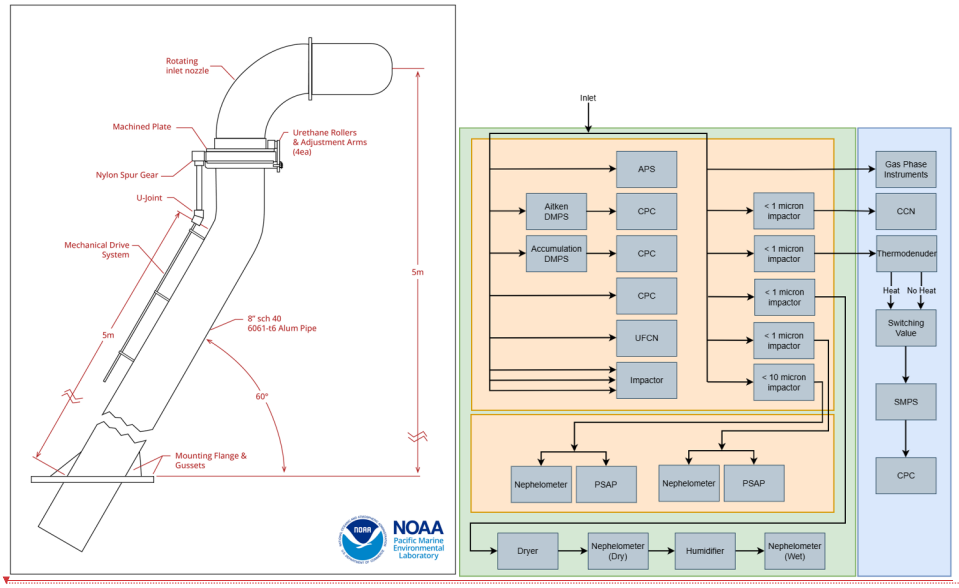

Deleted:

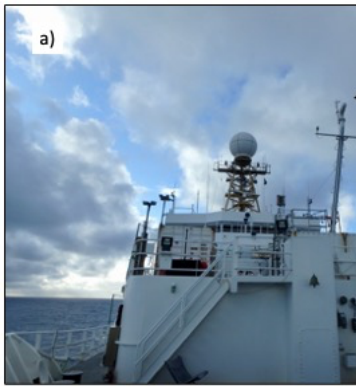

operated for 1 min every 5 min to maintain a steady concentration of ~ 500 particles per cm^3. Tests were conducted at different angles (0 to 90°) between the wind vector and the mast inlet cone axis, different wind speeds (7 to 20 m sec^{-1}), and different air flows down the mast (30 to 1200 l min^{-1}). The only parameter that was found to affect the transmission efficiency was the angle between the wind and the mast inlet cone. The transmission efficiency for particles with diameters less than 6.5 µm was determined to be greater than 95% when the inlet was kept to within 15° of the wind direction (Figure 3). At a 90° angle, the inlet transmitted about 60% of the particles in the 6 µm size bin. Data collected in bins greater than 6.5 µm were within the instrument noise level due to Poisson counting statistics.

Figure 3. Percent transmission efficiency of the mast at different angles between the inlet nozzle and the wind direction. The vertical bars indicate one standard deviation of the mean efficiency in each size bin. The curves are a second-order polynomial fit through the data at each angle. From Bates et al. (2002).

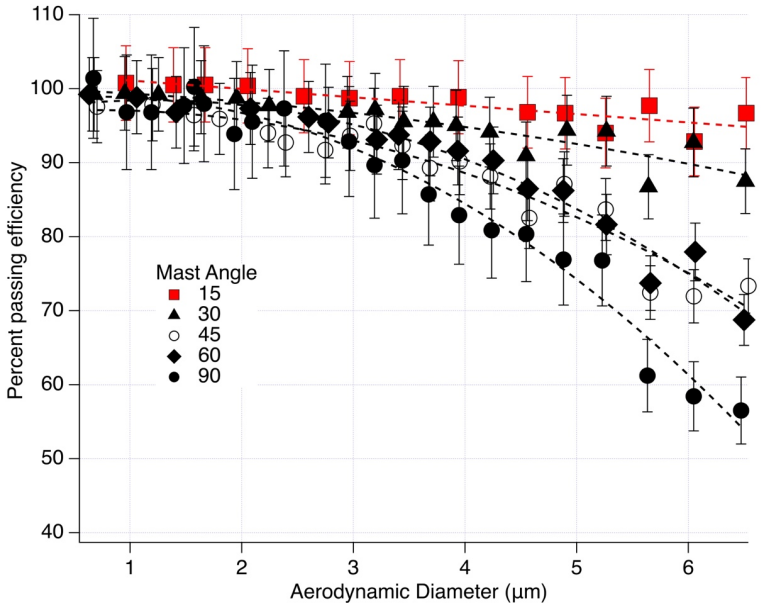

3.2. Aerosol microphysical properties

Total particle number concentration was measured on all cruises. After the first cruise, PSI-91, number size distributions were measured on all cruises. Measurements of cloud condensation nuclei (CCN) concentrations were first added in 2006 for TexAQS. Details of the measurements are outlined below. Table 2 indicates the measurement methods used on each cruise and, in the case of number size distributions, the instrumental RH.

3.2.1. Particle number concentrations

As indicated in Table 2, during the first several cruises (PSI-91, MAGE92, RITS93, RITS94), total particle number concentrations for D_p greater than 3 and 12 nm were measured with TSI 3025 and 3760 CPCs, respectively. The ultrafine particle number concentration was then defined as the difference between the number concentration measured with the 3025 and 3760 CPCs. For these initial cruises and all subsequent ones, diffusion driers (Permapure Inc.) were placed upstream of the CPCs to minimize particle diameter changes due to hygroscopic growth to less than 5% (Swietlicki et al., 2008). The use of a diffusion drier also helped prevent the uptake of water in the CPC condenser that results when sampling in the humid marine atmosphere. Beginning with ACE-2 in 1997 and continuing through ATOMIC in 2020, particle number concentrations for $D_p > 12$ nm were measured with a TSI 3010 CPC. Starting in 2008 for VOCALS, a water-based TSI 3785 CPC was added to also measure the concentrations of particles with diameters greater than 3 nm.

3.2.2. Particle number size distributions

For MAGE92, RITS93, and RITS94, particle number size distributions from 0.02 to 0.6 μm were measured with a TSI 3071 Differential Mobility Analyzer (DMA) (Quinn et al., 1998b) with the number concentration in each bin measured with a TSI 3760 CPC. The resulting number mobility distributions were inverted to a number size distribution by using the manufacturer-provided algorithm (Keady et al., 1983) and assuming that a Fuchs-Boltzman equilibrium charge distribution resulted from a Kr^{85} charge neutralizer (TSI model 3077) on the inlet of the DMA. The number concentration was corrected for the counting efficiency of the CPC (Zang et al., 1991) and diffusion losses in the DMA (Reineking et al., 1986). The sample air passed through a diffusion drier to reduce the RH to less than 25%.

A Vienna short column Ultrafine DMPS (UDMPS) coupled to a TSI 3025 CPC was added for ACE-1 and all subsequent cruises to extend the size distribution measurements to the 0.005 to 0.02 μm size range. For both ACE-1 and CSP, the UDMPS and the TSI 3071 DMA were located outside of the temperature-controlled box. Sheath air for both resulted in a measurement RH of less than 25% RH. As for the earlier

441 cruises, the mobility distributions were inverted to number size distributions by assuming that a Fuchs-
442 Boltzman charge distribution resulted from the Kr^{85} charge neutralizers on the inlet of the DMAs. The
443 data were corrected for diffusional losses (Covert et al., 1997) and size dependent counting efficiencies
444 (Wiedensohler et al., 1997) based on pre-ACE-1 intercalibration exercises. In addition, an APS (TSI
445 3300) was added for ACE-1 and all subsequent cruises to measure the number size distribution between
446 0.6 and 9.6 μm. APS diameters measured at ~ 40% RH were converted to geometric diameters by dividing
447 by the square root of the particle density for sea salt (1.9 g cm^{-3}) and dried to 10% RH assuming a sea salt
448 growth factor of 1.5 between 10 and 40% RH (Berg et al., 1998).
449
450 For ACE-2 and all subsequent cruises, the UDMPS and TSI DMA were put into the temperature-
451 controlled box to maintain an instrumental RH of greater than 45% (see Table 2). The APS was also
452 transferred to the temperature-controlled box where it measured at an RH of approximately 40%.
453
454 For AEROSOLS99 and all subsequent cruises, a Vienna medium column DMPS was used to measure
455 particles in the 0.02 – 0.9 μm size range instead of the TSI 3071 DMA. In addition, the APS model 3300
456 was replaced with an APS model 3320. Duplicate Vienna medium column DMPSs were deployed for
457 AEROSOLS99 and INDOEX. One measured at 10% RH outside of the temperature-controlled box and
458 the other measured at 55% RH inside the box.
459
460 Although the APS was located in the temperature-controlled box and its inlet was maintained at 55% RH,
461 internal heating of the sample flow by its sheath flow and waste heat likely reduced the measurement RH
462 (Bates et al., 2004). For ACE-Asia and all subsequent cruises, the APS sheath flow was routed outside of
463 the instrument to equilibrate with the air temperature in the temperature-controlled box and then
464 reintroduced to the sheath and acceleration nozzle to lower the temperature and increase the measurement
465 RH. Also starting with ACE-Asia, densities and the associated water masses at the instrumental RH were
466 calculated with a thermodynamic equilibrium model (AeRho) using the measured inorganic ion
467 composition (Quinn et al., 1998a). These calculated densities were used to convert the APS data from
468 aerodynamic to geometric diameters for merging with the DMPS data. Due to the atmospheric dust that

was sampled during ACE Asia, the APS data were corrected for ultra-Stokesian conditions in the instrument jet and nonspherical shape (Wang et al., 1987; Wang et al., 2002).

3.2.3. Cloud condensation nuclei concentrations

A CCN counter (DMT CCN-100) was added for TexAQS and several later cruises (CalNex, NAAMES-1, NAAMES-2, NAAMES-3, NAAMES-4, and ATOMIC) (see Table 2). A CCN counter was onboard during WACS and WACS2 but it sampled nascent SSA with Sea Sweep for the majority of the time. CCN concentrations were measured at supersaturations between 0.2 and 1.0%. Details of the CCN counter can be found in Roberts et al. (2005). A multijet cascade impactor (Berner et al., 1979) with a 50% aerodynamic cut-off diameter of 1.1 μm was upstream of the CCN counter. More details about the CCN measurements can be found in Quinn et al. (2008).

3.3. Aerosol chemical composition

The chemical species quantified along with sample collection and analysis methods are listed for each cruise in Table 3 and described below. Starting with PSI-91, size segregated aerosol was collected with a varying combination of two-, three-, and seven-stage multijet cascade impactors (Berner et al., 1979). All impactors, except those used for the analysis of organic carbon, had a grease cup at the inlet of the impactor that was coated with silicone grease to prevent the bounce of large particles onto the downstream stages. Two stage impactors had 50% aerodynamic cut-off diameters, $D_{aero,50}$, of 1.1 and 10 μm; three stage impactors had $D_{aero,50}$, of 0.18, 1.1, and 10 μm; and seven stage impactors had $D_{aero,50}$, of 0.18, 0.31, 0.55, 1.1, 2.0, 4.1, and 10 μm. To attain these size cuts, air flow through all impactors was maintained at 30 lpm. Flow through the impactors was computer-controlled so that aerosol was only collected when the relative wind speed and direction along with measured particle number concentration indicated there was no contamination from the ship's stack. Chemical analysis of the substrates included ion chromatography (inorganic ions), thermal/optical analysis (OC and EC), energy dispersive X-ray fluorescence (trace elements), and gravimetric mass (total aerosol mass). The substrates used in the impactors depended on the chemical species analyzed and are described below. Blank levels were determined by placing a substrate in the impactor with no air pulled through it. Blank concentrations were subtracted from sample

Table 2. Microphysical and cloud-nucleating properties measured on each cruise and the instrumentation used.

Measured parameter and method	Cruise
UFCN[a], D_p > 3 nm TSI 3025 CPC[b]	PSI-91, MAGE92, RITS93, RITS94, ACE-1, CSP, ACE-2, AEROSOLS99, INDOEX, NAURU99, ACE-Asia, NEAQS 2002, NEAQS 2004, TexAQS, ICEALOT
UFCN, D_p > 3 nm TSI 3785 CPC	VOCALS, CalNex, DYNAMO, WACS, WACS-2, NAAMES-1, NAAMES-2, NAAMES-3, NAAMES-4, ATOMIC
CN[c] > 12 nm TSI 3760 CPC	PSI-91, MAGE92, RITS93, RITS94
CN > 12 nm TSI 3010 CPC	ACE-2, AEROSOLS99, INDOEX, NAURU99, ACE-Asia, NEAQS 2002, NEAQS 2004, TexAQS, ICEALOT, VOCALS, CalNex, DYNAMO, WACS, WACS-2, NAAMES-1, NAAMES-2, NAAMES-3, NAAMES-4, ATOMIC
Number size distribution TSI 3071 DMA[d], 0.02 – 0.6 μm	MAGE92, RITS93, RITS94 (< 25% RH)
Number size distribution Vienna short column UDMPS[e], 0.005 – 0.02 μm TSI 3071 DMA, 0.02 – 0.6 μm TSI 3300 APS[f], 0.6 – 9.6 μm	ACE-1, CSP (< 25% RH); ACE-2 (45% RH)
Number size distribution Vienna short column UDMPS, 0.005 – 0.02 μm Vienna medium column DMPS[g], 0.02 – 0.9 μm TSI 3320 APS, 0.6 – 9.6 μm	AEROSOLS99, INDOEX (10 and 55% RH); NAURU99, ACE-Asia, NEAQS 2002, NEAQS 2004 (55% RH); TexAQS, VOCALS, CalNex, DYNAMO, CalNex, WACS, WACS-2, ATOMIC (60% RH); ICEALOT (< 25% RH); NAAMES-1, NAAMES-2, NAAMES-3, NAAMES-4 (<30 and 60% RH)
CCN[h] DMT CCN-100	TexAQS, ICEALOT, CalNex, NAAMES-1, NAAMES-2, NAAMES-3, NAAMES-4, ATOMIC

[a]Ultrafine Condensation Nuclei
[b]Condensation Particle Counter
[c]Condensation Nuclei
[d]Differential Mobility Analyzer
[e] Ultrafine Differential Mobility Particle Sizer
[f]Aerodynamic Particle Sizer
[g]Differential Mobility Particle Sizer
[h]Cloud Condensation Nuclei

concentrations.

Additional chemical analyses were performed with a particle-into-liquid-sampler (PILS) followed by ion chromatography and water soluble organic carbon (WSOC) analysis and an aerosol mass spectrometer (AMS) for non-refractory (NR) analytes. Details are provided below.

3.3.1. Inorganic ions

A seven stage multi-jet cascade impactor was used on all cruises to collect size segregated samples for ion chromatography analysis. The ions quantified were Na^+, NH_4^+, K^+, Ca^{2+}, Mg^{2+}, Cl^-, NO_3^-, $SO_4^=$, and methane sulfonate or MSA^-. A Millipore Fluoropore filter (1.0 μm pore size) was used for the final, smallest size range stage. The Millipore filter has a collection efficiency of 99% or greater for particles with diameters larger than 0.035 μm (Liu et al., 1976). Tedlar films were used for the six largest stages. The films were cleaned in an ultrasonic bath in 10% H_2O_2 for 30 min, rinsed 6 times in distilled, deionized water, and then dried in an NH_3- and SO_2-free glove box. Material collected on the filters and films was extracted by wetting with 1 mL of methanol and then adding 5 mL of distilled deionized water and sonicating for 30 min. Samples were handled in a glove box that was purged with air that had passed through a scrubber containing potassium carbonate, citric acid, and activated charcoal to remove SO_2, NH_3, and volatile organics, respectively. Sampling times varied between ~12 and 36 hrs and were based on the amount of aerosol present.

For the first few cruises (MAGE92, RITS93, RITS94), higher time resolution (< 12 hrs) submicron aerosol samples were collected using a filter holder downstream of a cyclone with a $D_{aero,50}$ of 1 μm. Starting with ACE-1, a 2-stage impactor was used for higher time resolution sampling of sub- and supermicron aerosol for ion chromatography analysis. Substrates, sample handling, and blank determinations were the same as discussed above.

A Particle-Into-Liquid-Sampler (PILS) coupled to an ion chromatograph was used to sample submicron inorganic ions during NEAQS 2002, NEAQS 2004, and TexAQS at a higher time resolution (15 min)

Deleted: $^{2-}$

than any of the impactors (Bates et al., 2008). The common aerosol inlet was used to deliver aerosol to a PILS at 55% RH. An impactor with a $D_{aero,50}$ of 1.1 um was upstream of the PILS. Flow through the impactor was 30 slpm with 15 slpm through the PILS and 15 slpm through a bypass line. Two annular, glass denuders (URG) were in series downstream of the impactor and upstream of the PILS. One was coated with sodium carbonate for the removal of gas phase acids and the other was coated with citric acid to remove gas phase bases. Two Kloehn syringe pumps were used to deliver a solution of LiF to the top of the PILS impactor to correct for dilution of the sample within the PILS. Two additional pumps delivered sample from the PILS simultaneously to a cation and an anion IC. More information about the PILS can be found in (Weber et al., 2001). Between every 45 min to 2 hrs, sample air was passed through a HEPA filter for 15 min to remove particles and determine the measurement blank. This blank was subtracted from the sample concentrations.

For both the impactor and the PILS data, non-sea salt (nss) $SO_4^=$ concentrations were calculated from Na^+ concentrations and the ratio of sulfate to sodium in seawater. Sea salt concentrations were calculated from

$$\text{Sea salt } (\mu g\ m^{-3}) = Cl^- (\mu g\ m^{-3}) + Na^+ (\mu g\ m^{-3}) \times 1.47 \quad (1)$$

where 1.47 is the seawater ratio of $(Na^+ + K^+ + Mg^{+2} + Ca^{+2} + SO_4^= + HCO_3^-)/Na^+$ (Holland, 1978). This approach prevents the inclusion of non-sea salt K^+, Mg^{+2}, Ca^{+2}, $SO_4^=$, and HCO_3^- in the sea salt mass and allows for the loss of Cl^- mass through Cl^- depletion processes. It also assumes that all measured Na^+ and Cl^- is derived from seawater. Results of Savoie et al. (1980) indicate that soil dust has a minimal contribution to measured soluble sodium concentrations.

3.3.2. Organic and Elemental Carbon

Starting with ACE-Asia in 2001, sub-1 and sub-10 μm samples were collected for OC/EC analysis using 2 and 1 stage impactors, respectively (Bates et al., 2004). Each impactor had 2 quartz backup filters. OC concentrations from both impactors were corrected for blanks and artifacts using the last quartz filter in line. Aluminum foil was used as a substrate on the 1.1 μm jet plate. All substrates, aluminum foil and

quartz, were prebaked at 500° prior to sampling. One sub-10 μm and one sub-1 μm impactor were operated without a denuder upstream to avoid losses of large particles in the denuder. OC from the sub-1μm impactor was subtracted from the OC from the sub-10 μm impactor to determine supermicron OC concentrations. A second sub-1 μm impactor was operated with a denuder upstream that contained strips of carbon-impregnated glass fiber filters to remove gas phase organics. Sub-1 μm OC and EC were quantified on the impactor samples downstream of the denuder.

During ACE-Asia and NEAQS 2002, a 7-stage impactor was used for the sampling of OC/EC providing greater size resolution. Aluminum foil substrates were used on all stages of the impactor along with 2 quartz backup filters. A 3-stage impactor ($D_{50,aero}$ of 0.18, 1.1, and 10 μm) was used during WACS, WACS-2, and NAAMES-1 through NAAMES-4. These cruises focused on the composition and properties of sea spray aerosol. The 3 size cuts allowed for the separation of the sub-0.18 μm aerosol from larger size ranges in recognition that smaller particle sizes are known to be enriched in organics through the sea spray aerosol production process (Keene et al., 2007).

OC and EC concentrations on the impactor substrates were measured with a Sunset Labs thermal/optical analyzer (Birch et al., 1996). Four temperature steps were used to achieve a final temperature of 870°C in He to drive off OC. After cooling the sample down to 550°C, a He/O_2 mixture was introduced and the sample was heated in four temperature steps to 910°C to drive off EC. The transmission of light through the filter was measured to separate EC from any OC that charred during the initial stages of heating. No correction was made for carbonate carbon so OC included both organic and inorganic carbon. The mass of particulate organic matter (POM) was determined by multiplying the measured organic carbon concentration in μg m^{-3} by a factor of 2.1 in marine regions and 1.6 elsewhere (Turpin et al., 2001).

A semi-continuous real-time Sunset Labs thermal/optical analyzer was used during NEAQS 2004 for higher time resolution measurements of OC concentrations. The OC/EC analyzer was downstream of a sub-1 μm impactor and a denuder. The analyzer collected air on a filter for 45 or 105 minutes depending

on OC concentrations. At the end of the sampling time the instrument analyzed the filter using the same temperature program described above. The sampling times were not long enough to measure EC above the detection limit of 0.35 μg m^{-3}.

3.3.3. Water soluble organic carbon

A PILS coupled to a Total Organic Carbon (TOC) analyzer (Sievers Model 800 Turbo) was used during TexAQS to measure water soluble organic carbon (WSOC) (Bates et al., 2008). As for the PILS-IC, the PILS-WSOC was connected to the common aerosol inlet but with a stainless steel line. An impactor with a $D_{50,aero}$ of 1.1 μm was upstream of the PILS to sample submicron aerosols. A denuder identical to the one used in the thermal/optical analysis was downstream of the impactor and upstream of the PILS to remove gas phase organics. Two syringe pumps (Kloehn) delivered low-TOC water to the top of the PILS impactor. Two additional pumps were used to pull sample out of the PILS and into the TOC analyzer. The sample was passed through a 0.5 μm in-line filter before entering the TOC analyzer to measure WSOC. Between every 45 min to 2 hrs, sample air was passed through a HEPA filter for 15 min to remove particles and determine the measurement background. The measurement background was subtracted from the sample air to obtain ambient WSOC ambient atmospheric concentrations.

3.3.4. Trace elements

Starting with AEROSOLS99, sub-1 and sub-10 μm samples were collected for trace element analysis using impactors with a $D_{50,aero}$ of 1.1 and 10 μm, respectively (Quinn et al., 2001). Energy Dispersive X-RAY Fluorescence (ED-XRF) was used for quantification (Buck et al., 2021). Both impactors collected aerosol on 2.0 μm pore size PALL Teflo Membrane Disc Filters. Supermicron concentrations were determined by subtracting the sub-1.1 μm values from the sub-10 μm values. No corrections were made for particle size or loading. Samples for XRF analysis were collected during all subsequent cruises except for VOCALS, WACS, WACS-2, and NAAMES-1 to 4.

Concentrations of Al, Si, Ca, Fe, and Ti are included in the NCEI archive as these were used to calculate dust. Other trace elements were measured but were often below detection limit so they were not reported.

Dust concentrations were calculated based on measured values of Al, Si, Ca, Fe, and Ti assuming that each element was present in the aerosol in its most common oxide form (Al_2O_3, SiO_2, CaO, K_2O, FeO, Fe_2O_3, TiO_2) (Seinfeld, 1986)). The measured elemental mass concentration was multiplied by the appropriate molar correction factor as shown below (Malm et al., 1994)

$$\text{Dust}=2.2(\text{Al}) + 2.49(\text{Si}) + 1.63(\text{Ca}) + 2.42(\text{Fe}) + 1.94(\text{Ti}). \quad (2)$$

This equation includes a 16% correction factor to account for the presence of oxides of other elements such as K, Na, Mn, Mg, and V that are not included in the linear combination. In addition, the equation omits K from biomass burning by using Fe as a surrogate for soil K and an average K/Fe ratio of 0.6 in soil (Braaten et al., 1986). Non-crustal K was calculated using the K/Al ratio (0.31) of Asian loess (Jahn et al., 2001) which is similar to the ratio in Saharan dust (0.24) and average crustal rock (0.32) (Formenti et al., 2003). Sea salt Ca was accounted for based on the ratio of Ca to Na in seawater.

3.3.5. Non-refractory species

Concentrations of submicron non-refractory (NR) NH_4^+, $SO_4^=$, NO_3-, and particulate organic matter (POM) were measured on NEAQS 2004, TexAQS, ICEALOT, VOCALS, CalNex, DYNAMO, WACS and WACS-2 with a Quadrupole Aerosol Mass Spectrometer (Q-AMS, Aerodyne Research Inc., Billerica, MA, USA) (Jayne et al., 2000). The NR species measured by the AMS are defined here as all the chemical components that vaporize at 550°C. The AMS was downstream of an impactor with a $D_{50,aero}$ of 1.1 µm. The ionization efficiency of the AMS was calibrated every few days with dry monodisperse ammonium nitrate particles. Particle losses due to transmission through the aerodynamic lens were corrected by using the DMPS and APS-measured size distributions. Particle losses due to bounce off of the impactor-vaporizer were corrected using simultaneously sampled NH_4^+ and non-sea salt $SO_4^=$ concentrations from either the PILS-IC or the impactors (Quinn et al., 2008; Quinn et al., 2006).

3.3.6. Aerosol Mass

Deleted: Concentrations of d

A filter holder with a Millipore Fluoropore filter (1.0 μm pore size) collected aerosol downstream of a cyclone with a $D_{50,aero}$ of 1 μm during RITS93 and RITS94. Filters were taken back to PMEL for gravimetric analysis to determine total submicron aerosol mass. The filters were weighed before and after sample collection with a Mettler UMT2 microbalance. The microbalance was housed in a glove box maintained at a constant RH to allow each sampled filter to come into equilibrium with the same vapor pressure of water, thus reducing experimental uncertainty due to a variable lab RH. For RITS93 and RITS94 the RH was maintained at less than 30% by circulating air through a flat baffle box containing a saturated solution of $M_gCl{\bullet}6H_2O$ and then through the glove box (Young, 1967). The circulated air was cleaned by passing it through a scrubber containing activated charcoal, potassium carbonate, and citric acid. Filters were equilibrated overnight in the glove box prior to weighing. Static charging, which can result in balance instabilities, was minimized by coating the walls of the glove box with a static dissipative polymer (Tech Spray, Inc.), placing an antistatic mat on the glove box floor, and exposing the filters to a ^{210}Po source to dissipate any built-up charge.

For ACE-1 and the other cruises listed in Table 3, a 2-stage impactor was used to collect submicron and supermicron aerosol for gravimetric analysis. Millipore Fluoropore filter (1.0 μm pore size) and Tedlar films were used for the collection of submicron and supermicron aerosol, respectively. The Tedlar films were cleaned as described in Section 3.3.1. prior to sample collection. Both the Millipore filters and the Tedlar films were weighed before and after sampling. Millipore filters were weighed on the Mettler UMT2 microbalance and Tedlar films were weighed on a Cahn Model 29 microbalance. Both balances were housed in the RH-controlled glove box described above. For cruises with higher sampling RHs of 55 to 60% (see Section 3.1.), a saturated solution of KBr was used in the baffle box.

In addition to the 2-stage impactor used during ACE-Asia, a 7-stage impactor was used for higher size resolution total aerosol mass concentrations.

All reported mass concentrations include the water mass that is associated with the aerosol on the filter at the glove box RH.

679 ***Table 3. Measurements of aerosol chemical composition on each cruise and the instrumentation used.***

Chemical Species and Measurement Method	Size range	Cruise
Inorganic ions		
Inorganic ions[a] Filter with cyclone upstream, IC[b]	Sub-1 μm	MAGE92, RITS93, RITS94
Inorganic ions 2-stage impactor, IC	Sub-1 μm, Supermicron	ACE-1, CSP, ACE-2, AEROSOLS99, INDOEX, NAURU99, ACE-Asia, NEAQS 2002, NEAQS 2004, TexAQS, ICEALOT, VOCALS, CalNex, DYNAMO, WACS, WACS-2, NAAMES-1, NAAMES-2, NAAMES-3, NAAMES-4, ATOMIC
Inorganic ions 7-stage impactor, IC	$D_{50,aero}$ of 0.18, 0.31, 0.55, 1.1, 2.0, 4.1, and 10 μm	All cruises
Inorganic ions PILS[c], IC	Sub-1 μm	NEAQS 2002, NEAQS 2004, TexAQS
Organic and Elemental Carbon		
OC and EC 2-stage impactor, Thermal analysis[d]	Sub-1 μm, Supermicron	ACE-Asia, NEAQS 2002, NEAQS 2004, TexAQS, ICEALOT, CalNex, ATOMIC
OC and EC Semi-continuous real-time OC/EC with impactor upstream[e], Thermal analysis	Sub-1 μm	NEAQS 2004
OC and EC 3-stage impactor, Thermal analysis	$D_{50,aero}$ of 0.18, 1.1, and 10 μm	WACS, WACS-2, NAAMES – 1, NAAMES-2, NAAMES-3, NAAMES-4
OC and EC 7-stage impactor, Thermal analysis	$D_{50,aero}$ of 0.18, 0.31, 0.55, 1.1, 2.0, 4.1, and 10 μm	ACE-Asia, NEAQS 2002
WSOC[f] PILS, TOC[g] analyzer	Sub-1 μm	TexAQS
Trace Elements		
Trace Elements[h] 2 impactors, XRF[i]	Sub-1 μm; Sub-10 μm	AEROSOLS99, INDOEX, ACE-Asia, NEAQS 2002, NEAQS 2004, TexAQS, ICEALOT, CalNex, DYNAMO, ATOMIC
Aerosol Mass		
Aerosol mass Filter with cyclone upstream, Gravimetric analysis	Sub-1 μm, Supermicron	RITS93, RITS94
Aerosol mass 2-stage impactor, Gravimetric analysis	Sub-1 μm, Supermicron	ACE-1, ACE-2, AEROSOLS99, INDOEX, ACE-Asia, NEAQS 2002, NEAQS 2004, TexAQS, ICEALOT, VOCALS, CalNex, DYNAMO, WACS, WACS-2, ATOMIC
Non-refractory Species		

NR[j] SO_4, NH_4, NO_3, POM, submicron AMS[k]	Sub-1 µm	NEAQS 2004, TexAQS, ICEALOT, VOCALS, CalNex, DYNAMO, WACS, WACS-2

[a] Na^+, NH_4^+, K^+, Ca^{2+}, Mg^{2+}, Cl^-, NO_3^-, $SO_4^{=}$, MSA^-

[b] Ion Chromatography

[c] Particle-Into-Liquid-Sampler

[d] Sunset Labs thermal/optical analyzer

[e] Sunset Labs real-time, semi-continuous thermal/optical analyzer

[f] Water Soluble Organic Carbon

[g] Total Organic Carbon Sievers Model 800 Turbo analyzer

[h] Al, Si, nss Ca, Ti, Fe

[i] Energy dispersive X-ray fluorescence

[j] Non-refractory

[k] Aerodyne Mass Spectrometer

Deleted: $^{2-}$

3.4. Aerosol optical Properties

The optical properties measured on each cruise and the instrumentation used are listed in Table 4. Aerosol light scattering coefficients were measure on each cruise with the exception of the first one, PSI-91. Variations included measurement at a single wavelength (550 nm) or three wavelengths (450, 550, and 700 nm) and measurement of sub-10 micron aerosol or sub-1 and sub-10 micron aerosol. The relative humidity dependence of light scattering, f(RH), was measured on some of the cruises as were backscattering coefficients at 450, 550, and 700 nm.

Aerosol absorption coefficients were measured on every cruise starting with ACE-1. Initially, measurements were made at 550 nm for sub-10 micron aerosol. These measurements were expanded to sub-1 and sub-10 micron aerosol starting with NAURU99 and 3 wavelengths (467, 530, and 660 nm) starting with NEAQS 2002.

Aerosol optical depth (AOD) was measured on all cruises except for the first one, PSI-91, with handheld sunphotometers. In addition, the NASA AMES Airborne Tracking sunphotometer (AATS-6) (Livingston et al., 2000) was used during ACE-2.

Details of the measurements are provided in the following sections.

712 **3.4.1. Aerosol Light Scattering**

713 During RITS93 and RITS94, sub-10 micron aerosol light scattering was measured with a newly
714 developed, highly sensitive multiwavelength integrating nephelometer (Bodhaine et al., 1991). This
715 nephelometer, with its high sensitivity, was combined with the closed geometry of the Ahlquist et al.
716 (1967) nephelometer to develop the TSI, Inc. model 3563 (Anderson et al., 1996) that was used during
717 the rest of the cruises reported on here. The enclosed geometry allows for the calibration of the
718 nephelometer with gases with known scattering coefficients.

719

720 The TSI Inc. model 3563 integrating nephelometer was used for all remaining cruises to measure sub-1
721 and sub-10 micron scattering at three wavelengths (450, 550, and 700 nm). Sub-1 and sub-10 micron
722 backscattering were measured on cruises between ACE-1 and WACS. Two single-stage impactors, one
723 having a $D_{50,aero}$ of 1.1 μm and the other of 10 μm were placed upstream of the nephelometer. A valve
724 automatically switched between the two impactors every 15 minutes so that sampling alternated between
725 sub-1 micron and sub-10 micron aerosol. Scattering and backscattering by the supermicron aerosol was
726 determined by difference.

727

728 During all cruises, the nephelometer was calibrated with CO_2 and zeroed with particle-free air every 3 to
729 4 days (Quinn et al., 1996). The resulting zero offset and span factors were applied to the data. In addition,
730 data were corrected for angular nonidealities of the nephelometer, including truncation errors and non-
731 Lambertian illumination using the method of Anderson et al. (1998) or one similar to it.

732

733 The RH of the air sampled by the nephelometer was nominally that of the common inlet as described in
734 Section 3.1. Heating within the nephelometer likely led to slightly lower RH's than for the sizing
735 instruments detailed in Table 2. For ACE-Asia and all subsequent cruises the nephelometer flow path was
736 modified so that the sheath flow was conditioned outside of the instrument case to equilibrate with the
737 temperature-controlled box. It was then reintroduced into the sheath and acceleration nozzle to minimize
738 heating of the sample air and lowering of the measurement RH. In addition, an RH sensor was placed in
739 the nephelometer sensing volume.

740

741 **3.4.2. Relative Humidity Dependence of Light Scattering, f(RH)**

742 As indicated in Table 4, the relative humidity dependence of scattering, f(RH), was measured on TexAQS,
743 ICEALOT, VOCALS, CalNex, DYNAMO, WACS, WACS-2, NAAMES-1, NAAMES-2, and
744 ATOMIC. A humidity-controlled system measured light scattering at two different relative humidities,
745 ~20% and ~85%, with two nephelometers operated in series downstream of an impactor
746 (D_{50},aero = 1.1 μm). The first nephelometer in line measured sample air dried with a PermaPure, multiple-
747 tube nafion dryer (model PR-94). Downstream of this nephelometer a humidifier was used to add water
748 vapor to the sample flow using 6 microporous Teflon tubes surrounded by a heated water-jacket.
749 Humidity was measured using a chilled mirror dew point hygrometer downstream of the second
750 nephelometer in line. The same calibration procedure described in Section 3.4.2. was used (Quinn et al.,
751 2022).

752

753 **3.4.3. Aerosol Light Absorption**

754 Between ACE-1 and INDOEX, the aerosol light absorption coefficient of sub-10 μm was measured with
755 a Particle Soot Absorption Photometer (PSAP, Radiance Research) at a wavelength of 550 nm and ~55%
756 RH. Measured values were corrected for a scattering artifact, the deposit spot size, flow rate, and the
757 manufacturer's calibration (Bond et al., 1999). Beginning with NAURU99, the absorption coefficient was
758 measured for sub-1 and sub-10 μm aerosol with the PSAP located downstream of the same impactors as
759 the nephelometer. For NEAQS 2002 and all subsequent cruises, a modified PSAP was used to measure
760 light absorption at three wavelengths (467, 530, and 700 nm) close to that of the TSI nephelometer for
761 calculation of single scattering albedo (Virkkula et al., 2005). Beginning with TexAQS and all following
762 cruises, a PermaPure nafion dryer was placed upstream of the PSAP so that the sample air was at ~25%
763 RH. Measurement of dry air was found to reduce instrument noise.

764

765 **3.4.4. Aerosol Optical Depth**

766 Handheld sunphotometers were used to measure AOD for ACE-1 and all subsequent cruises. A single
767 wavelength (550 nm) sunphotometer was used for ACE-1. A microtops unit (Solar Light Co.) was used

for all other cruises measuring at 380, 440, 500, 675, and 870 nm. Units were calibrated before each cruise by either Solar Light Co. or NASA Goddard Space Flight Center (GSFC) using a Langley plot approach (Shaw, 1983). Initially, a NASA Sensor Intercomparison and Merger for Biological and Interdisciplinary Oceanic Studies (SIMBIOS) MATLAB routine was used to convert raw signal voltages to AOD. Included in the conversion is a correction for Rayleigh scattering (Penndorf, 1957) and air mass to account for the curvature of the Earth (Kasten et al., 1989). Beginning with ICEALOT in 2008, data were reduced as part of NASA's Maritime Aerosol Network (Smirnov et al., 2009).

Table 4. Measurements of aerosol optical properties on each cruise and the instrumentation used.

Optical Property and Measurement Method	Size Range	Cruise
Scattering		
Scattering (550 nm[a]), Integrating nephelometer	Sub-10 micron	RITS93, RITS94
Scattering (450, 550, 700 nm), Integrating nephelometer, TSI Model 3563	Sub-1 and sub-10 micron	ACE-1, CSP, ACE-2, AEROSOLS99, INDOEX, NAURU99, ACE-Asia, NEAQS 2002, NEAQS 2004, TexAQS, ICEALOT, VOCALS, CalNex, DYNAMO, WACS, WACS-2, NAAMES-1, NAAMES-2, NAAMES-3, NAAMES-4, ATOMIC
Backscattering		
Backscattering (450, 550, 700 nm), Integrating nephelometer, TSI Model 3563	Sub-1 and sub-10 micron	ACE-1, CSP, ACE-2, AEROSOLS99, INDOEX, NAURU99, ACE-Asia, NEAQS 2002, NEAQS 2004, TexAQS, ICEALOT,VOCALS, CalNex, DYNAMO, WACS
Absorption		
Absorption (550 nm), PSAP[b], Radiance Research	Sub-10 micron	ACE-1, ACE-2, AEROSOLS99, INDOEX
Absorption (550 nm), Sub-1 and PSAP[b], Radiance Research	Sub-10 micron	NAURU99, ACE-Asia
Absorption (467, 530, 660 nm), PSAP[b]	Sub-1 and sub-10 micron	NEAQS 2002, NEAQS 2004, TexAQS, ICEALOT, VOCALS, CalNex, DYNAMO, WACS, WACS-2, NAAMES-1, NAAMES-2, NAAMES-3, NAAMES-4, ATOMIC
f(RH) scattering and backscattering		
f(RH), scattering and backscattering (450, 550, 700 nm) (25 and 85% RH) 2 Integrating nepelometers, TSI Model 3563	Sub-1 micron	TexAQS, ICEALOT, VOCALS, CalNex, DYNAMO, WACS, WACS-2, NAAMES-1, NAAMES-2, ATOMIC

AOD		
AOD (391, 500 nm) Handheld sunphotometer		RITS93, RITS94
AOD (375, 500, 778, 862 nm) Handheld sunphotometer		ACE-1
AOD (380, 450, 525, 864, 1021 nm) AATS-6[c], NASA AMES		ACE-2
AOD (380, 440, 500, 675, 870 nm) Handheld sunphotometer, Solar Light Co. Microtops		AEROSOLS99, INDOEX, NAURU99, ACE-Asia, NEAQS 2002, NEAQS 2004, TexAQS, ICEALOT, VOCALS, CalNex, DYNAMO, WACS, WACS-2, ATOMIC

[a]nm, wavelength
[b]Particle Soot Absorption Photometer
[c]Ames Airborne Tracking Sunphotometer

3.5. Gas phase species

Gas phase species that were measured include O_3, SO_2, Radon, and DMS. The cruises each gas was measured on and the measurement methods used are listed in Table 5. O_3 and SO_2 were measured primarily as tracers of pollution. Radon (as Rn^{222}) was measured as an indicator of contact of the sampled air with land (Whittlestone et al., 1998b). DMS was measured due to its link to nss $SO_4^{=}$ and MSA via oxidation in the atmosphere (e.g. Andreae et al. (1985)).

3.5.1. Ozone

O_3 was measured on all cruises with the exception of NAURU99 and WACS. Three different ozone UV analyzers were used over the years including a Dasibi 1008-AH UV photometer, a TECO Model 49 O_3 Analyzer, and a TECO Model 49C O_3 Analyzer (Table 5). For all cruises, a ¼" ID Teflon sample line was used to draw air from the top of the aerosol common sampling mast to the O_3 instrument located in the lab container at the base of the mast. The loss of O_3 in a Teflon sampling line is approximately 5% per 30 m indicating that losses were negligible (< 3%). At intervals of 1 to 4 days, a charcoal filter was placed in the sampling line for 1 hour to determine a zero which was subtracted from the O_3 signal. More details can be found in Johnson et al. (1990).

3.5.2. Sulfur dioxide

SO_2 was measured during ACE-Asia, NEAQS 2002, NEAQS 2004, TexAQS, ICEALOT, VOCALS, and CalNex with a Thermo Environmental Instruments Model 43C trace level pulsed fluorescence analyzer. Air was drawn through the 18 m aerosol common sampling mast at 1 m^3 min^{-1}. At the base of the mast, a 5.0 L min^{-1} flow was pulled in series through a 1 m long Teflon tube, a Millipore Fluoropore Teflon filter (1.0 μm pore size), a Perma Pure Inc. Nafion dryer (MD-070), a 2 m long Teflon tube, and then into the SO_2 analyzer. The initial 1 m of tubing, filter, and drier were located in the humidity-controlled box at the base of the mast. Dry air was pulled through a charcoal trap and then through the outside of the Nafion dryer at 2 L min^{-1}. The analyzer was run with two channels (0 – 20 ppb full scale and 0 – 100 ppb full scale) and a 20 sec averaging time.

Zero air (scrubbed with a charcoal trap) was introduced into the sample line upstream of the Fluoropore filter for 10 min every hour to establish a zero baseline. An SO_2 standard was generated with a permeation tube held at 50°C. The flow over the permeation tube, diluted to 17.7 ppb, was introduced into the sample line upstream of the Fluoropore filter for 10 min every 6 hrs (Bates et al., 2004).

3.5.3. Radon

The rate of emission of radon from the ocean is ~ 100 times less than over land. As a result, ^{222}Rn is a qualitative tracer of an air mass that has been recently influenced by continental emissions (Carlson et al., 1972).

Radon was measured on all cruises starting with ACE-1 except AEROSOL99, INDOEX, NAURU99, and DYNAMO. Radon (^{222}Rn – half-life of 3.82 days) was measured using the two-filter detector method of Whittlestone et al. (1998a). Air is drawn through a HEPA filter which removes all radon and thoron decay products (i.e., daughters), then through a delay chamber in which some daughters are produced. Finally, the air passes through a second filter which retains the daughters. These daughters have been produced in controlled conditions so their number is proportional to the radon concentration. A photomultiplier then counts the radon daughters produced in a 750 L decay tank for a 30-min period. The

detector was standardized using radon emitted from a dry radon source (RN-25, PylonElectronics Corp). Background counts were measured under conditions of zero air flow (Quinn et al., 2022).

3.5.4. DMS

Air and seawater samples for DMS were analyzed using an automated purge and trap system. Air samples were collected through a Teflon line which ran approximately 60 m from the top of the aerosol sampling mast to the instrument. One hundred mL min^{-1} of the 4 L min^{-1} flow were pulled through a KI solution at the instrument to eliminate oxidant interferences (Cooper et al., 1993). The air sample volume ranged from 0.5 to 1.5 L depending on the DMS concentration. Water vapor was removed by passing the flow through a -25°C Teflon tube filled with silanized glass wool. DMS was then trapped in another -25°C Teflon tube filled with Tenax. During the sample trapping period, methylethyl sulfide (MES) was added to the sample stream as an internal standard. At the end of the sampling/purge period, the coolant was pushed away from the trap and the trap was electrically heated. DMS was desorbed onto a DB-1 mega-bore fused silica column where the sulfur compounds were separated isothermally at 50°C quantified with either a Flame Photo Detector (FPD) or a Sulfur Chemiluminescence Detector (SCD). The instrument was calibrated gravimetrically with calibrated permeation tubes. More details of the analysis can be found in Bates et al. (1998b).

3.6. Seawater species

3.6.1. DMS

Seawater samples for DMS analysis were collected from the ship's seawater pumping system at a depth of approximately 5 m below the ship's waterline. Periodically, a 5 mL water sample was valved from the ship's water line into a Teflon gas stripper. The sample was purged with hydrogen for 5 min. DMS and other sulfur gases in the hydrogen purge gas were collected on the Tenax trap held at -25°C as for the air samples. Seawater and air sample analysis was identical.

3.6.2. NH_4^+ and NO_3^-

Seawater samples for the analysis of NH_4^+ and NO_3^- were taken from a depth of ~ 5 m using the ship's seawater pumping system. Samples were analyzed for NH_4^+ using the phenolhypochlorite colorimetric method of Solarzano (1969) and for NO_3^- using the method of Parsons et al. (1984). Both of the analyses were undertaken with a Technicon Autoanalyzer II (Technicon Corp., Tarrytown, New York).

3.6.3. Chlorophyll-a

Discrete seawater samples for chlorophyll-a analysis were taken from the ship's seawater pumping system 2 to 6 times per day. Samples were immediately filtered, put into 10 mL of 90% acetone, and frozen. Samples were analyzed with a fluorometer within 3 to 4 days onboard the ship. Depending on the cruise, the fluorometer was calibrated several times during, before, or after the experiment usually with algal chlorophyll 'a' (Sigma Chemical Corp.). The discrete samples were used to calibrate continuous fluorescence measurements of seawater also from the ship's underway seawater pumping system.

Table 5. Measurements of gas phase species on each cruise and the instrumentation used.

Parameter and Measurement Method	Cruise
Ozone	
O_3 Dasibi 1008-AH UV[a] Photometer	PSI-91, MAGE92, RITS93, RITS94, ACE-1, CSP, ACE-2, AEROSOLS99, INDOEX, ACE-Asia, NEAQS 2004
O_3 TECO Model 49 O_3 Analyzer	RITS94, ACE-1, CSP, ACE-2, AEROSOLS99, INDOEX, ACE-Asia, NEAQS 2002, NEAQS 2004,
O_3 TECO Model 49C O_3 Analyzer	TexAQS, ICEALOT, VOCALS, CalNex, DYNAMO, WACS, WACS-2, NAAMES-1, NAAMES-2, NAAMES-3, NAAMES-4, ATOMIC
SO_2	
SO_2 TEI Model 43C SO_2 Analyzer	ACE-Asia, NEAQS 2002, NEAQS 2004, TexAQS, ICEALOT, VOCALS, CalNex
Radon	
Radon (^{222}Rn) Two-filter Radon Detector	ACE-1, CSP, ACE-2, ACE-Asia, ACE-Asia, NEAQS 2002, NEAQS 2004, TexAQS, ICEALOT, VOCALS, CalNex, WACS, WACS-2, NAAMES-1, NAAMES-2, NAAMES-3, NAAMES-4, ATOMIC
DMS	
Atmospheric DMS Purge-and-trap system with FPD[b]	MAGE92, RITS93

[a]Ultra-Violet
[b]Flame Photometric Detector

[c]Sulfur Chemiluminesence Detector

Table 6. Measurements of seawater species on each cruise and the instrumentation used.

Parameter and Measurement Method	Cruise
Seawater DMS Purge-and-trap system with FPD	PSI-91, MAGE92, RITS93
Seawater DMS Purge-and-trap system with SCD	RITS94, ACE-1, CSP, ACE-2, AEROSOLS99, INDOEX, ACE-Asia, NEAQS 2004, TexAQS, ICEALOT, VOCALS, CalNex, WACS, WACS-2
Seawater NH_4^+ Technicon Autoanalyzer II	RITS94
Seawater NO_3- Technicon Autoanalyzer II	PSI-91, RITS93, RITS94, ACE-1, CSP, AEROSOLS99, INDOEX, NAURU99
Seawater Chlorophyll-a Fluorometer	PSI-91, RITS93, RITS94, ACE-1, CSP, ACE-2, AEROSOLS99, INDOEX, NAURU99, CalNex, WACS, WACS-2, NAAMES-1, NAAMES-2, NAAMES-3, NAAMES-4, ATOMIC

3.7. Ancillary parameters

Ancillary meteorological and seawater parameters were routinely measured on all cruises. These parameters include latitude, longitude, ship's speed and course, true wind speed and direction, relative wind speed and direction, ambient temperature and relative humidity, barometric pressure, and rain rate. Radiosonde data are available for all cruises except PSI-91, MAGE92, RITS93, RITS94, DYNAMO, and WACS. Seawater parameters include sea surface temperature and salinity.

4 Summary of Major Findings

Listed below are many of the high-level major findings reported by PMEL based on its global ocean data set of marine aerosol properties. Although they may seem fundamental now, they are a result of early foundational measurements built upon over time with additional cruises in different parts of the world's

oceans. These findings were not developed solely by PMEL but along with other pioneering shipboard and aircraft measurements made by many other researchers.

1. **Measurements of key sulfur species in surface seawater show that most seawater DMS is microbially consumed in the water column, while the ocean-to-atmosphere flux of DMS is a minor sink in the seawater sulfur cycle** (Bates et al., 1994) (Data from PSI-91).
2. **The mean surface seawater DMS concentration in the equatorial Pacific (15°S to 15°N) is relatively constant seasonally and interannually**. Large interannual variations associated with El Nino – Southern Oscillation (ENSO) events appear to have little effect on the concentration of DMS in tropical surface ocean waters (Bates et al., 1994). (Data from MAGE92, RITS93, RITS94, ACE-1, CSP and previous cruises not described here).
3. **New particle production in the marine boundary layer is rare** due to the high surface area of sea salt aerosol resulting in the condensation of gas phase precursors onto existing aerosol (Quinn et al., 1993; Covert et al., 1996; Bates et al., 1998b). (Data from PSI-91, MAGE92, RITS93, RITS94, ACE-1).
4. **The marine aerosol number size distribution has modal characteristics that depend on large scale meteorological features and marine boundary layer residence times**. Strong subsidence and entrainment from the FT produce an aerosol dominated by particles in the ultra – fine and Aitken modes (~ 2 to 80 nm). Residence time in the MBL of a few days or more results in a bimodal aerosol with Aitken and accumulation modes (80 to 300 nm in diameter) (Covert et al., 1996; Quinn et al., 1996; Bates et al., 1998b; Bates et al., 2000; Bates et al., 2001; Bates et al., 2002; Quinn et al., 2017). (Data from MAGE92, RITS93, RITS94, ACE-1, ACE-2, AEROSOL99, ICEALOT, WACS-2, NAAMES-1).
5. **Regional and mesoscale meteorological transport patterns impact aerosol number and volume distributions, chemical composition, and optical and cloud-nucleating properties** (Bates et al., 2001; Bates et al., 2002; Bates et al., 2004; Bates et al., 2008; Quinn et al., 2022). (Data from ACE-1, ACE-2, AEROSOLS99, ACE-Asia, NEAQS 2002, NEAQS 2004, TexAQS, ATOMIC).

6. Sea salt can comprise a significant mass fraction of not only supermicron but also submicron aerosol in the marine atmosphere. Its relatively large mass concentration, high scattering efficiency, and lifetime comparable to other submicron chemical components often results in **submicron sea salt being the dominant contributor to submicron scattering in the marine boundary layer** (Quinn et al., 1996; Quinn et al., 1998b; Murphy et al., 1998; Quinn et al., 1999; Quinn et al., 2000; Quinn et al., 2005a). (Data from PSI-91, MAGE92, RITS93, RITS94, ACE-1, ACE-2, AEROSOLS99, INDOEX, ACE-Asia, CSP, NEAQS 2002).
7. **Instantaneous wind speed often only accounts for a small fraction of the variance in the coarse mode number concentration (~30%) and sea salt submicron and supermicron mass concentrations (~20 to 78%)** due to variability in upwind conditions and advection to the measurement location (Bates et al., 1998b; Quinn et al., 1999). (Data from PSI-91, MAGE92, RITS93, RITS94, ACE-1).
8. **A variable and often large fraction of submicron aerosol mass in the marine boundary layer, both remote and continentally influenced, is composed of species other than non-sea salt sulfate** (Mcinnes et al., 1996; Quinn et al., 2000; Quinn et al., 2005a). (Data from PSI-91, MAGE92, RITS93, RITS94, ACE-1, ACE-2, AEROSOLS99, INDOEX, ACE-Asia, CSP, NEAQS 2002)**.**
9. **Sea salt makes up a small fraction of marine boundary layer cloud condensation nuclei** (Quinn et al., 2017; Quinn et al., 2019). **Instead, the CCN population between 70°S and 80°N is composed primarily of nss $SO_4^=$** due to large-scale meteorological features that result in entrainment of particles from the FT into the MBL and regionally varying MBL aerosol residence times. (Data from RITS93, RITS94, ACE-1, ICEALOT, WACS-2, NAAMES-1, NAAMES-2, NAAMES-3, NAAMES-4).
10. **Particulate organic matter and its degree of oxidation impacts the relative humidity dependence of light scattering and aerosol cloud nucleation** (Quinn et al., 2005b; Quinn et al., 2008). (Results from INDOEX, ACE-Asia, NEAQS 2002, TexAQS).

5 Data Set Usage

Examples of previous uses of the data based on PMEL co-authorship are listed below. Future use of the data is likely to be similar but could be expanded, for example, to halogen chemistry relating to sea spray aerosol.

1. **Constraints on models and parameterizations** (e.g., Global distribution of sea salt aerosols: new constraints from in situ and remote observations (Jaegle et al., 2011); A review of sea-spray aerosol source functions using a large global set of sea salt aerosol concentration measurements (Gyrthe et al., 2014); Atmospheric sulfur cycle simulated in the global model GOCART' Comparison with field observations and regional budgets (Chin et al., 2000); Modelled radiative forcing of the direct aerosol effect with multi-observation evaluation (Myhre et al., 2009); Numerical study of Asian dust transport during the springtime of 2001 simulated with the Chemical Weather Forecasting System (CFORS) model (Uno et al., 2004); CCN predictions using simplified assumptions of organic aerosol composition and mixing state: a synthesis from six different locations (Ervens et al., 2010); A model for the radiative forcing during ACE-Asia derived from CIRPAS Twin Otter and R/V Ronald H. Brown data and comparison with observations (Conant et al., 2003); Global sea-salt modeling: Results and validation against multicampaign shipboard measurements (Witek et al., 2007); The Global Aerosol Synthesis and Science Project (GASSP) (Reddington et al., 2017)).

2. **Intercomparison of instruments and methods** (e.g., ACE-Asia intercomparison of a thermal-optical method for the determination of particle-phase organic and elemental carbon (Schauer et al., 2003); Bias in filter based aerosol absorption measurements due to organic aerosol loading: Evidence from ambient measurements (Lack et al., 2008); Comparison of aerosol single scattering albedos derived by diverse techniques in two North Atlantic experiments (Russell et al., 2002)).

3. **Comparison to and validation of remote retrievals** (e.g., Measurements of aerosol vertical profiles and optical properties during INDOEX 1999 using micropulse lidars (Welton et al., 2002);

Geostationary satellite retrievals of aerosol optical thickness during ACE-Asia (Wang et al., 2003); Clear-sky infrared aerosol radiative forcing at the surface and the top of the atmosphere (Markovic et al., 2003); Spectral absorption of solar radiation by aerosols during ACE-Asia (Bergstrom et al., 2004); Lidar measurements during Aerosols99 (Voss et al., 2001); Multi-grid-cell validation of satellite aerosol property retrievals in INTEX/ITCT/ICARTT 2004 (Russell et al., 2007); Shipboard sunphtometer measurements of aerosol optical depth spectra and columnar water vapor during ACE 2 and comparison with selected land, ship, aircraft, and satellite measurements).

4. **Addition to larger data sets** (e.g., Maritime aerosol network as a component of aerosol robotic network (Smirnov et al., 2009); Total observed organic carbon (TOOC) in the atmosphere: a synthesis of North American observations (Heald et al., 2008); A global database of sea surface DMS measurements and a simple model to predict sea surface DMS as a function of latitude, longitude and month (Kettle et al., 1999)).

6 Summary

PMEL conducted 25 cruises between 1991 and 2020 measuring aerosol chemical, microphysical, optical, and cloud nucleating properties. These cruises provide coverage in all of the world's oceans resulting in the largest global ocean data set of marine aerosol properties. The data set also includes gas phase and seawater species. PMEL's major findings and data usage by others are summarized. A description of each cruise is provided including location, timing, and objectives. References are cited to provide a deeper context for each cruise. The intention of the paper is to advance widespread use of the data by the broader research community.

7 Data availability

All cruise data sets are publicly available at NOAA's National Centers for Environmental Information (https://www.ncei.noaa.gov). Cruise identification, data links (DOIs), and data references are provided in Table 6. The data are permanently and publicly available at NCEI.

998

999 ***Table 6. Summary of cruise data links (DOIs), and references. See Table 1 for dates, ports, and ocean***
1000 ***region for each cruise. The data are permanently and publicly available at NOAA's NCEI.***
1001

Cruise	Data links	Data reference
PSI-91	https://doi.org/10.25921/44nn-d608	(Quinn et al., 2026c)
MAGE92	https://doi.org/10.25921/bz8f-b917	(Quinn et al., 2026k)
RITS93	https://doi.org/10.25921/ec4p-9410	(Quinn et al., 2026h)
RITS94	https://doi.org/10.25921/ec4p-9410	(Quinn et al., 2026h)
ACE-1 Leg 1	https://doi.org/10.25921/z3bm-y330	(Quinn et al., 2026g)
ACE-1 Leg 2	https://doi.org/10.25921/z3bm-y330	(Quinn et al., 2026g)
CSP	https://doi.org/10.25921/pgzy-5h08	(Quinn et al., 2026f)
ACE-2	https://doi.org/10.25921/3fk0-0m36	(Quinn et al., 2025f)
AEROSOLS99	https://doi.org/10.25921/67kx-2d82	(Quinn et al., 2026b)
INDOEX	https://doi.org/10.25921/67kx-2d82	(Quinn et al., 2026b)
NAURU99	https://doi.org/10.25921/e2rz-yg88	(Quinn et al., 2026i)
ACE-Asia	https://doi.org/10.25921/jd13-t245	(Quinn et al., 2026j)
NEAQS 2002	https://doi.org/10.25921/q66h-r438	(Quinn et al., 2026l)
NEAQS 2004	https://doi.org/10.25921/q66h-r438	(Quinn et al., 2026l)
TexAQS-GoMACCS	https://doi.org/10.25921/c6n1-0840	(Quinn et al., 2025a)
ICEALOT	https://doi.org/10.25921/bgy4-3075	(Quinn et al., 2025c)
VOCALS	https://doi.org/10.25921/mafn-2n04	(Quinn et al., 2025e)
CalNex	https://doi.org/10.25921/xf4m-dx08	(Quinn et al., 2025b)
DYNAMO	https://doi.org/10.25921/m0ec-rn58	(Quinn et al., 2026e)
WACS	https://doi.org/10.25921/tx5t-1e17	(Quinn et al., 2026d)
WACS2	https://doi.org/10.25921/tx5t-1e17	(Quinn et al., 2026d)
NAAMES1	https://doi.org/10.25921/df6d-p183	(Quinn et al., 2025d)
NAAMES2	https://doi.org/10.25921/df6d-p183	(Quinn et al., 2025d)
NAAMES3	https://doi.org/10.25921/df6d-p183	(Quinn et al., 2025d)
NAAMES4	https://doi.org/10.25921/df6d-p183	(Quinn et al., 2025d)

ATOMIC	https://doi.org/10.25921/w7ab-3s87	(Quinn et al., 2026a)

Author contributions

T.S.B. and P.K.Q. conceptualized research goals. P.K.Q., T.S.B., D.J.C., J.E.J., and L.M.U. participated in collecting and analyzing data. P.K.Q. prepared the paper. D.J.C. and H.B. prepared data sets for archival at NCEI.

Competing interests

The authors declare that they have no conflict of interest.

Acknowledgments

We thank the crews of the NOAA *R/Vs* Discoverer, Surveyor, and Ronald H. Brown; USC *R/V* Vickers; the IBSS *R/V* Professor Vodyanitiskiy; and UNOLS *R/Vs* Atlantis, Roger Revelle, and Knorr who made this work possible. This is PMEL contribution number 5806.

Financial support

Funding was provided over the years by NOAA's Climate and Global Change Program, New England Air Quality Study, Health of the Atmosphere Program, Climate Program Office, and Oceanic and Atmospheric Research Office; NASA's Interdisciplinary Studies Program, Mission to Planet Earth Science Division, Global Aerosol Climatology Project, and Earth System Science Program; the NSF Atmospheric Chemistry Program; and the Office of Naval Research.

References

Ahlquist, N. C. and Charlson, R. J.: A new instrument for evaluating the visual quality of air, Journal of the Air Pollution Control Association, 17, 467 - 469., 1967.

Aller, J., Radway, J. C., Kilthau, W. P., Bothe, D. W., Wilson, T. W., Vaillancourt, R. D., Quinn, P. K., Coffman, D. J., et al.: Size-resolved characterization of the polysaccharided and proteinaceous components of seawater, Atmospheric Environment, 154, 331 - 347, 2017.

1032 Anderson, T. L. and Ogren, J.: Determining aerosol radiative properties using the TSI 3563 integrating
1033 nephelometer, Aerosol Science and Technology, 29, 57 - 69, 1998.

1034 Anderson, T. L., Covert, D. S., Marshall, S. F., Laucks, M. L., Charlson, R. J., Waggoner, A. P., Ogren,
1035 J., Caldow, R., et al.: Performance characteristics of a high-sensitivity, three-wavelength total
1036 scatter/backscatter nephelometer, Journal of Atmospheric and Oceanic Technology, 13, 967 - 986,
1037 1996.

1038 Andreae, M. O., Ferek, R. J., Bermond, F., Byrd, K. P., Engstrom, T., Hardin, S., Houmere, P. D.,
1039 LeMarrec, F., et al.: Dimethyl sulfide in the marine atmosphere, Journal of Geophysical Research -
1040 Atmosphere, 90, 12,891 - 812,900, 1985.

1041 Bates, T. S., Coffman, D. J., Covert, D. S., and Quinn, P. K.: Regional marine boundary layer aerosol
1042 size distributions in the Indian, Atlantic and Pacific Oceans: A comparison of INDOEX measurements
1043 with ACE-1 and ACE-2, and Aerosols99, Journal of Geophysical Research - Atmospheres, 107, 8026,
1044 2002.

1045 Bates, T. S., Quinn, P. K., Coffman, D. J., and Johnson, J. E.: The Dominance of Organic Aerosols in
1046 the Marine Boundary Layer over the Gulf of Maine during NEAQS 2002 and their Role in Aerosol
1047 Light Scattering, Journal of Geophysical Research - Atmosphere, 110, doi:10.1029/2005JD005797,
1048 2005.

1049 Bates, T. S., Huebert, B. J., Gras, J., Griffiths, F. B., and Durkee, P. A.: International Global
1050 Atmospheric Chemistry (IGAC) Projects' First Aerosol Characterization Experiment (ACE 1):
1051 Overview, Journal of Geophysical Research - Atmosphere, 103, 16,297 - 216,318, 1998a.

1052 Bates, T. S., Quinn, P. K., Coffman, D. J., Johnson, J. E., Miller, T. L., and Covert, D. S.: Regional
1053 physical and chemical properties of the marine boundary layer aerosol across the Atlantic during
1054 Aerosols99: An overview, Journal of Geophysical Research - Atmosphere, 106, 20,767 - 720,782, 2001.

1055 Bates, T. S., Quinn, P. K., Coffman, D. J., Schulz, K., Covert, D. S., and Johnson, J. E.: Boundary Layer
1056 Aerosol Chemistry during TexAQS/GoMACCS 2006: Insights into Aerosol Sources and
1057 Transformation Processes, Journal of Geophysical Research - Atmosphere, 113,
1058 doi:10.1029/2008JD010023, 2008.

1059 Bates, T. S., Quinn, P. K., Covert, D. S., Coffman, D. J., Johnson, J. E., and Wiedensohler, A.: Aerosol
1060 physical properties and processes in the lower marine boundary layer: A comparison of shipboard sub-
1061 micron data from ACE-1 and ACE-2, Tellus, 52B, 258 - 272, 2000.

1062 Bates, T. S., Kiene, R. P., Wolfe, G. V., Matrai, P. A., Chavez, F. P., Buck, K. R., Blomquist, B. W.,
1063 and Cuhel, R. L.: The cycling of sulfur in surface seawater of the northeast Pacfic, Journal of
1064 Geophysical Research - Atmospheres, 99, 7835 - 7843, 1994.

1065 Bates, T. S., Kapustin, V. N., Quinn, P. K., Covert, D. S., Coffman, D. J., Mari, C., Durkee, P. A., De
1066 Bruyn, W., and Saltzman, E. S.: Processes controlling the distribution of aerosol particles in the lower
1067 marine boundary layer during the First Aerosol Characterization Experiment (ACE 1), Journal of
1068 Geophysical Research - Atmosphere, 103, 16,369 - 316,383, 1998b.

1069 Bates, T. S., Quinn, P. K., Coffman, D. J., Covert, D. S., Miller, T. L., Johnson, J. E., Carmichael, G.
1070 R., Guazotti, S. A., et al.: Marine boundary layer dust and pollution transport associated with the
1071 passage of a frontal system over eastern Asia, Journal of Geophysical Research - Atmosphere, 109,
1072 doi:10.1029/2003JD004094, 2004.

1073 Bates, T. S., Quinn, P. K., Frossard, A. A., Russell, L. M., Hakala, J., Petaja, T., Kulmala, M., Covert,
1074 D. S., et al.: Measurements of ocean derived aerosol off the coast of California, Journal of Geophysical
1075 Research-Atmospheres, 117, Artn D00v15
1076 Doi 10.1029/2012jd017588, 2012.

1077 Behrenfeld, M. J., Moore, R. H., Hostetler, C. A., Graff, J., Gaube, P., Russell, L. M., Chen, G., Doney,
1078 S. C., et al.: The North Atlantic aerosol and marine ecosystem study (NAAMES): Science motive and
1079 mission overview, Frontiers of Marine Science, 22, doi.org/10.3389/fmars.2019.00122, 2019.

1080 Berg, O. H., Swietlicki, E., and Krejci, R.: Hygroscopic growth of the aerosol particles in the marine
1081 boundary layer over the Pacfic and Southern Oceans during the First Aerosol Characterization
1082 Experiment (ACE 1), Journal of Geophysical Research - Atmosphere, 103, 16,535 - 516,546, 1998.

1083 Bergstrom, R. W., Pilewskie, P., Schmid, B., Redemann, J., Russell, P. B., Hiragashi, A., Nakajima, T.,
1084 and Quinn, P. K.: Spectral absorption of solar radiation by aerosols during ACE-Asia, Journal of
1085 Geophysical Research - Atmosphere, 109, doi:10.1029/2003JD004467, 2004.

1086 Berner, A., Lurzer, C., Pohl, F., Preining, O., and Wagner, P.: The size distribution of the urban aerosol
1087 in Vienna, Science of the Total Environment, 13, 245 - 261, 1979.

1088 Birch, M. E. and Cary, R. A.: Elemental carbon-based method for monitoring occupational exposures to
1089 particulate diesel exhaust, Aerosol Science and Technology, 25, 221 - 241, 1996.

1090 Bodhaine, B. A., Alhquist, N. C., and Schnell, R. C.: Three-wavelength nephelometer suitable for
1091 aircraft measurements os background aerosol scattering extinction coefficient, Atmospheric
1092 Environment, 25A, 2267 - 2276, 1991.

1093 Bond, T. C., Anderson, T. L., and Campbell, D.: Calibration and intercomparison of filter-based
1094 measurements of visible light absorption by aerosols, Aerosol Science and Technology, 30, 582 - 600,
1095 1999.

1096 Braaten, D. A. and Cahill, T. A.: Size and composition of Asian dust transported to Hawaii,
1097 Atmospheric Environment, 20, 1105 - 1109, 1986.

Buck, N. J., Barrett, P. M., Morton, P. L., Landing, W. M., and Resing, J. A.: Energy dispersive X-ray fluorescence methodology and analysis of suspended particulate matter in seawater for trace element compositions and an intercomparison with high-resolution inductively coupled plasma-mass spectrometry, Limnology and Oceanography: Methods, 19, 401 - 415, 2021.

Carlson, T. N. and Prospero, J. M.: The large-scale movement of Saharan air outbreaks over the northern equatorial Atlantic, Journal of Applied Meteorology, 11, 283 - 297, 1972.

Carrico, C. M., Kus, P., Rood, M. J., Quinn, P. K., and Bates, T. S.: Mixtures of pollution, dust, sea salt, and volcanic aerosol during
ACE-Asia: Aerosol radiative properties as a function of relative humidity, Journal of Geophysical Research - Atmosphere, 108, doi:10.1029/2003JD003405, 2003.

Charlson, R. J., Pueschel, R. F., and Horvath, H.: The direct measurement of atmospheric light scattering coefficient for studies of visibility and air pollution, Atmospheric Environment, 1, 469 - 478, 1967.

Chin, M., Savoie, D. L., Huebert, B. J., Bandy, A. R., Thornton, D. C., Bates, T. S., Quinn, P. K., Saltzman, E. S., and De Bruyn, W.: Atmospheric sulfur cycle simulated in the global model GOCART: Comparison with field observations and regional budgets, Journal of Geophysical Research - Atmosphere, 105, 24,689 - 624,712, 2000.

Clarke, A. D., Freitag, S., Simpson, R. M. C., Hudson, J. G., Howell, S. G., V.L., B., Campos, T., and Kapustin, V. N.: Free troposphere as a major source of CCN for the equatorial pacific boundary layer: long-range transport and teleconnections, Atmospheric Chemistry and Physics, 13, 7511 - 7529, 2013.

Conant, W. C., Seinfeld, J. H., Wang, J., Carmichael, G. R., Tang, Y., Uno, I., Flatau, P. J., Markowicz, K. M., and Quinn, P. K.: A model for the radiative forcing during ACE-Asia derived from CIRPAS

1120 Twin Otter and R/V Ronald H. Brown data and comparison with observations, Journal of Geophysical
1121 Research - Atmosphere, 108, doi:10.1029/2002JD003260, 2003.

1122 Cooper, D. J. and Saltzman, E. S.: Measurements of atmospheric dimethylsulfide, hydrogen sulfide, and
1123 carbon disulfide during GTE/CITE 3, Journal of Geophysical Research - Atmosphere, 98, 23,397 -
1124 323,410, 1993.

1125 Corbett, J. J., Winebrake, J. J., Green, E. H., Kasibhatla, P., Eyring, V., and Lauer, A.: Mortality from
1126 ship emissions: A global assessment, Environmental Science & Technology, 41, 8512-8518, Doi
1127 10.1021/Es071686z, 2007.

1128 Covert, D. S., Wiedensohler, A., and Russell, L. M.: Particle charging and transmission efficiencies of
1129 aerosol charge neutralizers, Aerosol Science and Technology, 27, 206 - 214, 1997.

1130 Covert, D. S., Kapustin, V. N., Bates, T. S., and Quinn, P. K.: Physical properties of marine boundary
1131 layer aerosol particles of the mid-Pacific in relation to sources and meteorological transport, Journal of
1132 Geophysical Research - Atmosphere, 101, 6919 - 6930, 1996.

1133 Covert, D. S., Kapustin, V. N., Quinn, P. K., and Bates, T. S.: New particle formation in the marine
1134 boundary layer, Journal of Geophysical Research - Atmosphere, 97, 20,581 - 520,590, 1992.

1135 de Leeuw, G., Andreas, E. L., Anguelova, M. D., Fairall, C. W., Lewis, E. R., O'Dowd, C., Schulz, M.,
1136 and Schwartz, S. E.: Production Flux of Sea Spray Aerosol, Reviews of Geophysics, 49, Rg2001,
1137 10.1029/2010rg000349, 2011.

1138 DeWitt, H. L., Coffman, D. J., Schulz, K. J., Brewer, A., Bates, T. S., and Quinn, P. K.: Atmospheric
1139 aerosol properties over the equatorial Indian Ocean and the impact of the Madden-Julia Oscillation,
1140 Journal of Geophysical Research - Atmospheres, 118, 10.1002/jgrd.50419, 2013.

1141 Ervens, B., Cubison, M. J., Andrews, E., Feingold, G., Ogren, J., Jimenez, J., Quinn, P. K., Bates, T. S.,
1142 et al.: CCN predictions using simplified assumptions of organic aerosol composition and mixing state: a
1143 synthesis from six different locations, Atmospheric Chemisty and Physics, 10, 4795 - 4807, 2010.

1144 Fehsenfeld, F. C., Ancellet, G., Bates, T. S., Goldstein, A. J., Hardesty, R. M., Honrath, R., Law, K. S.,
1145 Lewis, A. C., et al.: International Consortium for Atmospheric Research on Transport and
1146 Transformation (ICARTT): North America to Europe —Overview of the 2004 summer field study,
1147 Journal of Geophysical Research - Atmospheres, 111, 10.1029/2006JD0078729, 2006.

1148 Formenti, P., Elbert, W., Maenhaut, W., Haywood, J., and Andreae, M. O.: Chemical composition of
1149 mineral dust aerosol during the Saharan Dust Experiment (SHADE) airborne campaign in the Cape
1150 Verde region, September 2000, Journal of Geophysical Research - Atmosphere, 108,
1151 https://doi.org/10.1029/2002JD002648, 2003.

1152 Gyrthe, H., Strom, J., Krejci, R., Quinn, P. K., Coffman, D. J., and Eck, T. F.: A review of seaspray
1153 aerosol source functions using a large global set of sea salt aerosol concentration measurements,
1154 Atmospheric Chemisty and Physics, 14, 1277 - 1297, 2014.

1155 Hawkins, L. N. and Russell, L. M.: Polysaccharides, Proteins, and Phytoplankton Fragments: Four
1156 Chemically Distinct Types of Marine Primary Organic Aerosol Classified by Single Particle
1157 Spectromicroscopy, Advances in Meteorology, 612132, 10.1155/2010/612132, 2010.

1158 Heald, C. L., Goldstein, A. H., Allan, J., Aiken, A. C., Apel, E., Atlas, E. L., Baker, A. K., Bates, T. S.,
1159 et al.: Total observed organic carbon (TOOC) in the atmosphere: a synthesis of North American
1160 observations, Atmospheric Chemisty and Physics, 8, 2007 - 2025, 2008.

1161 Holland, H. D.: The Chemistry of the Atmosphere and Oceans, John Wiley, New York1978.

1162 Huebert, B. J., Bates, T. S., Russell, P. B., Shi, G., Kim, Y. J., Kawamura, K., Carmichael, G., and
1163 Nakajima, T.: An overview of ACE-Asia: Strategies for quantifying the relationships between Asian
1164 aerosols and their climatic impacts, Journal of Geophysical Research - Atmospheres, 108,
1165 10.1029/2003JD003550, 2003.

1166 Jaegle, L., Quinn, P. K., Bates, T. S., Alexander, B., and Lin, J. T.: Global distribution of sea salt
1167 aerosols: new constraints from in situ and remote sensing observations, Atmospheric Chemistry and
1168 Physics, 11, 3137-3157, DOI 10.5194/acp-11-3137-2011, 2011.

1169 Jahn, B.-M., Gallet, S., and Han, J.: Geochemistry of the Xining, Xifeng and Jixian section, Loess
1170 Plateau of China: Eolian dust
1171 provenanceand paleosol evolution during the last 140 k, Chemical Geology, 178, 71 - 94, 2001.

1172 Jayne, J. T., Leard, D. C., Zhang, X., Davidovits, P., Smith, K. A., Kolb, C. E., and Worsnop, D. R.:
1173 Development of an aerosol mass spectrometer for size and composition analysis of submicron particles,
1174 Aerosol Science and Technology, 33, 49 - 70, 2000.

1175 Johnson, J. E., Gammon, R. H., Larsen, J., Bates, T. S., Oltmans, S. L., and Farmer, J. C.: Ozone in the
1176 marine boundary layer over the Pacific and Indian Oceans: Latitudinal Gradients and Diurnal Cycles,
1177 Journal of Geophysical Research - Atmosphere, 95, 11,847 - 811,856, 1990.

1178 Kasten, F. and Young, A. T.: Revised optical air mass tables and approximation formula, Applied
1179 Optics, 28, 4735 - 4738, 1989.

1180 Kaufman, Y. J., Koren, I., Remer, L., Tanre, D., Ginoux, P., and Fan, S.: Dust transport and deposition
1181 observed from the Terra-Moderate Resolution Imaging Spectroradiometer (MODIS) spacecraft over the
1182 Atlantic Ocean
1183 , Journal of Geophysical Research - Atmospheres, 110, doi:10.1029/2003JD004436, 2005.

1184 Kawamura, K., Hoque, M., Bates, T. S., and Quinn, P. K.: Molecular distributions and isotopic
1185 compositions of organic aerosols over the western North Atlantic: Dicarboxylic acids, related
1186 compounds, sugars and secondary organic aerosol tracers, Organic Geochemistry, 113, 229 - 238, 2017.

1187 Keady, P. B., Quant, F. R., and Sem, G. S.: Differential mobility particle sizer: A new instrument for
1188 high resolution aerosol size distribution measurements below 1 micron, TSI Q., 9, 3 - 11, 1983.

1189 Keene, W. C., Long, M. S., Reid, J. S., Frossard, A. A., Kieber, D. J., Maben, J., Russell, L. M., Kinsey,
1190 J. D., et al.: Factors that modulate properties of primary marine aerosol generated from ambient
1191 seawater on ships at sea, Journal of Geophysical Research - Atmospheres, 122, 11,961 - 911,990, 2017.

1192 Keene, W. C., Maring, H., Maben, J. R., Kieber, D. J., Pszenny, A. A. P., Dahl, E. E., Izaguirre, M. A.,
1193 Davis, A. J., et al.: Chemical and physical characteristics of nascent aerosols produced by bursting
1194 bubbles at a model air-sea interface, Journal of Geophysical Research-Atmospheres, 112, D21202,
1195 10.1029/2007jd008464, 2007.

1196 Kettle, A. J., Andreae, M. O., Amouroux, D., Andreae, T. W., and Bates, T. S.: A global database of sea
1197 surface dimethylsulfide (DMS) measurements and a simple model to predict sea surface DMS as a
1198 function of latitude, longitude and month, Global Biogeochemical Cycles, 13, 399 - 444, 1999.

1199 Lack, D. A., Cappa, C. D., Covert, D. S., Baynard, T., Passoli, P., Sierau, G., Bates, T. S., Quinn, P. K.,
1200 et al.: Bias in filter based aerosol absorption measurements due to organic aerosol loading: Evidence
1201 from ambient measurements, Journal of Aerosol Science and Technology, 42,
1202 doi:10.1080/02786820802389277, 2008.

1203 Li, J., Carlson, B. E., Yung, Y. L., Lv, D., Hansen, J., Penner, J., Liao, H., Ramaswamy, V., et al.:
1204 Scattering and absorbing aerosols in the climate system, Nature Reviews Earth and Environment, 3, 363
1205 - 379, 2022.

1206 Liu, B. Y. H. and Lee, K. W.: Efficiency of membrane and Nuclepore filters for submicrometer
1207 aerosols, Environmental Science and Technology, 10, 345 - 350, 1976.

1208 Livingston, J. M., Kapustin, V. N., Schmid, B., Russell, P. B., Quinn, P. K., Bates, T. S., Durkee, P. A.,
1209 Smith, P. J., et al.: Shipboard sunphotometer measurements of aerosol optical depth spectra and
1210 columnar water vapor during ACE-2 and comparison with selected land, ship, aircraft, and satellite
1211 measurements, Tellus, 52B, 594 - 619, 2000.

1212 Logan, T., Xi, B., Dong, X., Obrecht, R., Li, Z., and Cribb, M.: A study of Asian dust plumes using
1213 satellite, surface, and aircraft measurements during the INTEX-B field experiment, Journal of
1214 Geophysical Research - Atmospheres, 115, doi.org/10.1029/2010JD014134, 2010.

1215 Malm, W. C., Sisler, J. F., Huffman, D., Eldred, R. A., and Cahill, T. A.: Spatial and seasonal trends in
1216 particle concentration and optical extinction in the United States, Journal of Geophysical Research -
1217 Atmosphere, 99, 1347 - 1370, 1994.

1218 Markovic, M. Z., Flatau, P. J., Vogelmann, A. M., Quinn, P. K., and Welton, E. J.: Clear-sky infrared
1219 aerosol radiative forcing at the surface and the top of the atmosphere, Quarterly Journal of the Royal
1220 Meteorological Society, 129, 2927 - 2948, 2003.

1221 McInnes, L. M., Quinn, P. K., Covert, D. S., and Anderson, T. L.: Gravimetric analysis, ionic
1222 composition, and associated water mass of the marine aerosol, Atmospheric Environment, 30, 869 -
1223 884, 1996.

1224 Murphy, D. M., Anderson, J. R., Quinn, P. K., McInnes, L. M., Brechtel, F. J., Kreidenweis, S. M.,
1225 Middlebrook, A. M., Posfai, M., et al.: Influence of sea-salt on aerosol radiative properties in the
1226 Southern Ocean marine boundary layer, Nature, 392, 62-65, 1998.

1227 Myhre, G., Berglen, T. F., Johnsrud, M., Hoyle, C. R., Bernsten, T. K., Christopher, S. A., Fahey, D.
1228 W., Isaksen, I., et al.: Modelled radiative forcing of the direct aerosol effect with multi-observation
1229 evaluation, Atmospheric Chemisty and Physics, 9, 1365 - 1392, 2009.

1230 Parrish, D. D., Allen, D. T., Bates, T. S., Estes, M., Fehsenfeld, F. C., Feingold, F., Ferrare, R.,
1231 Hardesty, R. M., et al.: Overview of the second Texas air quality study (TexAQS II) and the Gulf of
1232 Mexico atmospheric composition and climate study (GoMACCS), Journal of Geophysical Research -
1233 Atmospheres, 114, doi:10.1029/2009JD011842, 2009.

1234 Parsons, T. R., Maita, Y., and Lalli, C. M.: A Manual of Chemical and Biological Methods for Seawater
1235 Analysis, Pergamon, New York1984.

1236 Penndorf, R.: Tables of refractive index for standard air and the Rayleigh scattering coefficient for the
1237 spectral region between 0.2 and 20 um and their application to atmospheric optics, Journal of the
1238 Optical Society of America, 47, 176 - 182, 1957.

1239 Post, M. J. and Fairall, C. W.: Early results from the Nauru99 campaign on NOAA ship Ronald H.
1240 Brown, IGARS 2000, 110.1109/IGARSS.2000.85802,

1241 Post, M. J., Fairall, C. W., J.R., S., Han, Y., White, A. B., Ecklund, W. L., Weickmann, A., Quinn, P.
1242 K., et al.: The combined sensor program: an air-sea science mission in the central and western Pacific
1243 Ocean, Bulliten of the American Meteorological Society, 78, 2797 - 2815, 1997.

1244 Quinn, P. K. and Bates, T. S.: Regional aerosol properties: Comparisons of boundary layer
1245 measurements from ACE 1, ACE 2, Aerosols99, INDOEX, ACE Asia, TARFOX, and NEAQS, Journal
1246 of Geophysical Research - Atmosphere, 110, doi: 10/1024/2004JD004755, 2005a.

Quinn, P. K. and Coffman, D. J.: Local closure during ACE 1: Aerosol mass concentration and scattering and backscattering coefficients, Journal of Geophysical Research - Atmosphere, 109, 16575 - 16596, 1998a.

Quinn, P. K. and Coffman, D. J.: Comment on "Contribution of different aerosol species to the global aerosol extinction optical thickness: Estimates from model results" by Tegen et al., Journal of Geophysical Research-Atmospheres, 104, 4241-4248, Doi 10.1029/1998jd200066, 1999.

Quinn, P. K., Bates, T. S., and Coffman, D. J.: Texas Air Quality - Gulf of Mexico Atmospheric Composition and Climate Study (TexAQS/GoMACCS): Physical, optical, and chemical properties of atmospheric marine aerosols aboard NOAA R/V Ronald H. Brown in the Gulf of America, 2006-07-27 to 2006-09-12 (NCEI Accession 0310784). NOAA National Centers for Environmental Information. [dataset], https://doi.org/10.25921/c6n1-0840, 2025a.

Quinn, P. K., Bates, T. S., and Coffman, D. J.: California Research at the Nexus of Air Quality and Climate Change (CalNex) Field Campaign: Physical, optical, and chemical properties of atmospheric marine aerosols aboard WHOI R/V Atlantis along the California coast, 2010-05-14 to 2010-06-09 (NCEI Accession 0310783). NOAA National Centers for Environmental Information. [dataset], https://doi.org/10.25921/xf4m-dx08, 2025b.

Quinn, P. K., Bates, T. S., and Coffman, D. J.: International Chemistry Experiment in the Arctic Lower Troposphere (ICEALOT): Physical, optical, and chemical properties of atmospheric marine aerosols aboard WHOI R/V Knorr in Arctic ice-free regions of the Greenland, Norwegian, and Barents seas, 2008-03-19 to 2009-04-24 (NCEI Accession 0310737). NOAA National Centers for Environmental Information. [dataset], https://doi.org/10.25921/bgy4-3075, 2025c.

Quinn, P. K., Bates, T. S., and Coffman, D. J.: North Atlantic Aerosols and Marine Ecosystems Study (NAAMES): Physical, optical, and chemical properties of atmospheric marine aerosols aboard WHOI

R/V Atlantis in the western subarctic North Atlantic, 2015 to 2018 (NCEI Accession 0310822). NOAA National Centers for Environmental Information. [dataset], https://doi.org/10.25921/df6d-p183, 2025d.

Quinn, P. K., Bates, T. S., and Coffman, D. J.: VAMOS Ocean-Cloud-Atmosphere-Land Study - Regional Experiment (VOCALS-REx): Physical, optical, and chemical properties of atmospheric marine aerosols aboard NOAA R/V Ronald H. Brown in the tropical eastern Pacific, 2008-10-20 to 2008-12-01 (NCEI Accession 0310622). NOAA National Centers for Environmental Information. [dataset], https://doi.org/10.25921/mafn-2n04, 2025e.

Quinn, P. K., Bates, T. S., and Coffman, D. J.: The second Aerosol Characterization Experiment (ACE-2): Physical, optical, and chemical properties of atmospheric marine aerosols aboard IBSS R/V Vodyanitskiy in the subtropical northeast Atlantic, 1997-06-19 to 1997-07-23 (NCEI Accession 0311148). NOAA National Centers for Environmental Information. [dataset], https://doi.org/10.25921/3fk0-0m36, 2025f.

Quinn, P. K., Bates, T. S., and Coffman, D. J.: Atlantic Tradewind Ocean-Atmosphere Mesoscale Interaction Campaign (ATOMIC): Physical, optical, and chemical properties of atmospheric marine aerosols aboard NOAA R/V Ronald H. Brown in the tropical North Atlantic, 2020-01-07 to 2020-02-11 (NCEI Accession 0311369). NOAA National Centers for Environmental Information. [dataset], https://doi.org/10.25921/w7ab-3s87, 2026a.

Quinn, P. K., Bates, T. S., and Coffman, D. J.: Indian Ocean Experiment (INDOEX): Physical, optical, and chemical properties of atmospheric marine aerosols aboard NOAA R/V Ronald H. Brown in the Atlantic and Indian Oceans, 1999-01-14 to 1999-03-31 (NCEI Accession 0312108). NOAA National Centers for Environmental Information. [dataset], https://doi.org/10.25921/67kx-2d82, 2026b.

Quinn, P. K., Bates, T. S., and Coffman, D. J.: Pacific Sulfur-Stratus Investigation (PSI): Physical and chemical properties of atmospheric marine aerosols aboard NOAA R/V Discoverer off the coast of

Washington state, 1991-04-16 to 1991-05-01 (NCEI Accession 0311260), NOAA National Centers for Environmental Information. [dataset], https://doi.org/10.25921/44nn-d608, 2026c.

Quinn, P. K., Bates, T. S., and Coffman, D. J.: Western Atlantic Climate Study (WACS): Physical, optical, and chemical properties of atmospheric marine aerosols in Georges Bank and the Sargasso Sea aboard NOAA R/V Ronald H. Brown (2012-08-19 to 2012-08-28) and WHOI R/V Knorr (2014-05-20 to 2014-06-06) (NCEI Accession 0310824). NOAA National Centers for Environmental Information. [dataset], https://doi.org/10.25921/tx5t-1e17, 2026d.

Quinn, P. K., Bates, T. S., and Coffman, D. J.: Dynamics of the Madden-Julian Oscillation (DYNAMO) Field Campaign: Physical, optical, and chemical properties of atmospheric marine aerosols aboard SIO R/V Roger Revelle in the equatorial Indian ocean, 2011-10-01 to 2011-12-07 (NCEI Accession 0310825). NOAA National Centers for Environmental Information. [dataset], https://doi.org/10.25921/m0ec-rn58, 2026e.

Quinn, P. K., Bates, T. S., and Coffman, D. J.: Combined Sensor Program (CSP): Physical, optical, and chemical properties of atmospheric marine aerosols aboard NOAA R/V Discoverer in the central and tropical western Pacific, 1996-03-15 to 1996-04-12 (NCEI Accession 0311408). NOAA National Centers for Environmental Information. [dataset], https://doi.org/10.25921/pgzy-5h08, 2026f.

Quinn, P. K., Bates, T. S., and Coffman, D. J.: Aerosol Characterization Experiment (ACE-1): Physical, optical, and chemical properties of atmospheric marine aerosols aboard NOAA R/V Discoverer in the southern hemisphere, 1995-10-13 to 1995-12-13 (NCEI Accession 0311430). NOAA National Centers for Environmental Information. [dataset], https://doi.org/10.25921/z3bm-y330, 2026g.

Quinn, P. K., Bates, T. S., and Coffman, D. J.: Radiatively Important Trace Species (RITS) Field Campaign: Physical, optical, and chemical properties of atmospheric marine aerosols aboard NOAA R/V Surveyor in the central Pacific, 1993-03-20 to 1993-05-08 and 1993-11-21 to 1994-01-08 (NCEI

Accession 0310738). NOAA National Centers for Environmental Information. [dataset], https://doi.org/10.25921/ec4p-9410, 2026h.

Quinn, P. K., Bates, T. S., and Coffman, D. J.: NAURU-99 Field Campaign: Physical, optical, and chemical properties of atmospheric marine aerosols aboard NOAA R/V Ronald H. Brown in the southwestern Pacific, 1999-06-14 to 1999-07-16 (NCEI Accession 0311261). NOAA National Centers for Environmental Information. [dataset], https://doi.org/10.25921/e2rz-yg88, 2026i.

Quinn, P. K., Bates, T. S., and Coffman, D. J.: Asian Pacific Regional Aerosol Characterization Experiment (ACE-Asia): Physical, optical, and chemical properties of atmospheric marine aerosols aboard NOAA R/V Ronald H. Brown in the western Pacific, 2001-03-15 to 2001-04-20 (NCEI Accession 0311457). NOAA National Centers for Environmental Information. [dataset], https://doi.org/10.25921/jd13-t245, 2026j.

Quinn, P. K., Bates, T. S., and Coffman, D. J.: Marine Aerosol and Gas Exchange (MAGE-92) Field Campaign: Physical and chemical properties of atmospheric marine aerosols aboard NOAA R/V John Vickers in the tropical Pacific, 1992-02-21 to 1992-03-23 (NCEI Accession 0310736). NOAA National Centers for Environmental Information. [dataset], https://doi.org/10.25921/bz8f-b917, 2026k.

Quinn, P. K., Bates, T. S., and Coffman, D. J.: New England Air Quality Study (NEAQS): Physical, optical, and chemical properties of atmospheric marine aerosols aboard NOAA R/V Ronald H. Brown in the Gulf of Maine and the northwest Atlantic, 2002-07-12 to 2002-08-10 and 2004-07-05 to 2004-08-13 (NCEI Accession 0311433). NOAA National Centers for Environmental Information. [dataset], https://doi.org/10.25921/q66h-r438, 2026l.

Quinn, P. K., Bates, T. S., Coffman, D. J., and Covert, D. S.: Influence of particle size and chemistry on the cloud nucleating properties of aerosols, Atmospheric Chemisty and Physics, 8, 1029 - 1042, 2008.

Quinn, P. K., Kapustin, V. N., Bates, T. S., and Covert, D. S.: Chemical and optical properties of marine boundary layer aerosol particles of the mid-Pacific in relation to sources and meteorological transport, Journal of Geophysical Research - Atmosphere, 101, 6931 - 6951, 1996.

Quinn, P. K., Bates, T. S., Coffman, D. J., Upchurch, L. M., and Johnson, J. E.: Wintertime observations of tropical northwest Atlantic aerosol properties during ATOMIC: Varying mixtures of dust and biomass burning, Journal of Geophysical Research - Atmosphere, 127, doi: 10.1029/2021JD036253, 2022.

Quinn, P. K., Coffman, D. J., Johnson, J. E., Upchurch, L. M., and Bates, T. S.: Small fraction of marine cloud condensation nuclei made up of sea spray aerosol, Nature Geoscience, 10, 674 - 679, 2017.

Quinn, P. K., Coffman, D. J., Kapustin, V. N., Bates, T. S., and Covert, D. S.: Aerosol optical properties in the MBL during ACE-1 and the underlying chemical and physical aerosol properties, Journal of Geophysical Research - Atmosphere, 103, 16,547 - 516,564, 1998b.

Quinn, P. K., Collins, D. B., Grassian, V. H., Prather, K. A., and Bates, T. S.: Chemistry and related properties of freshly emitted sea spray aerosol, Chemical Reviews, doi:10.1021/cr500713g, 2015.

Quinn, P. K., Marshall, S., Bates, T. S., Covert, D. S., and Kapustin, V. N.: Comparison of measured and calculated aerosol properties relevant to the direct radiative forcing of tropospheric sulfate aerosol particles, Journal of Geophysical Research - Atmospheres, 100, 8977 - 8992, 1995.

Quinn, P. K., Covert, D. S., Bates, T. S., Kapustin, V. N., Ramsey-Bell, D. C., and McInnes, L. M.: Dimethylsulfide/cloud condensation nuclei/climate system: Relevant size-resolved measurements of the chemical and physical properties of atmospheric aerosol particles, Journal of Geophysical Research - Atmosphere, 98, 10,411 - 410,4227, 1993.

Quinn, P. K., Bates, T. S., Schultz, K. S., Coffman, D. J., Frossard, A. A., Russell, L. M., Keene, W. C., and Kieber, D. J.: Contribution of sea surface carbon pool to organic matter enrichment in sea spray aerosol, Nature Geoscience, 7, 228-232, 10.1038/ngeo2092, 2014.

Quinn, P. K., Coffman, D. J., Bates, T. S., Miller, T. L., Johnson, J. E., Voss, K. J., Welton, E. J., and Neusüß, C.: Dominant aerosol chemical components and their contribution to extinction during the Aerosols99
cruise across the Atlantic, Journal of Geophysical Research - Atmosphere, 106, 20,783 - 720,809, 2001.

Quinn, P. K., Bates, T. S., Coffman, D. J., Upchurch, L. M., Moore, R., Ziemba, L., Bell, T., Saltzman, E. S., et al.: Seasonal variations in western North Atlantic remote marine aerosol properties, Journal of Geophysical Research - Atmosphere, 124, 14,240 - 214,261, 2019.

Quinn, P. K., Bates, T. S., Miller, T. L., Coffman, D. J., Johnson, J. E., Harris, J. M., Ogren, J., Forbes, G., et al.: Surface submicron aerosol chemical composition: What fraction is not sulfate?, Journal of Geophysical Research - Atmospheres, 105, 6785 - 6805, 2000.

Quinn, P. K., Bates, T. S., Baynard, T., Clarke, A., Onasch, T. B., Wang, W., Rood, M. J., Andrews, E., et al.: Impact of particulate organic matter on the relative humidity dependence of light scattering: A simplified parameterization, Geophysical Research Letters, 32, doi:101029/2005GL024322, 2005b.

Quinn, P. K., Bates, T. S., Coffman, D. J., Onasch, T. B., Worsnop, D. R., Baynard, T., de Gouw, J. A., Goldan, P. D., et al.: Impacts of sources and aging on submicrometer aerosol properties in the marine boundary layer across the Gulf of Maine, Journal of Geophysical Research - Atmosphere, 111, doi:10.1029/2006JD007582, 2006.

Quinn, P. K., Thompson, E. J., Coffman, D. J., Baidar, S., Bariteau, L., Bates, T. S., Bigorre, S., Brewer, A., et al.: Measurements from the RV Ronald H. Brown and related platforms as part of the

1382 Atlantic Tradewind Ocean-Atmosphere Mesoscale Interaction Campaign (ATOMIC), Earth System
1383 Science Data, 13, 1759 - 1790, 2021.

1384 Raes, F., Bates, T. S., McGovern, F., and Vanliedekerke, M.: The Second Aerosol Characterization
1385 Experiment, Tellus, 52B, 111 - 125, 2000.

1386 Ramanathan and al., e.: Indian Ocean Experiment: An integrated analysis of the climate forcing effects
1387 of the great Indo-Asian haze, Journal of Geophysical Research - Atmospheres, 106, 28,371 - 328,398,
1388 2001.

1389 Reddington, C. L., Carslaw, K. S., Stier, P., Schutgens, N., Coe, H., Liu, D., Allan, J., Browse, J., et al.:
1390 The Global Aerosol Synthesis and Science Project (GASSP), Bulliten of the American Meteorology
1391 Society, 98, 1857 - 1877, 2017.

1392 Reineking, A. and Porstendorfer, J.: Measurements of particle loss functions in a differential mobility
1393 analyzer for different flow rates, Aerosol Science and Technology, 5, 483 - 487, 1986.

1394 Roberts, G. C. and Nenes, A.: A continuous-flow streamwise thermal-gradient CCN chamber for
1395 atmospheric measurements, Aerosol Science and Technology, 39, 206 - 221, 2005.

1396 Russell, L. M., Hawkins, L. N., Frossard, A. A., Quinn, P. K., and Bates, T. S.: Carbohydrate-like
1397 composition of submicron atmospheric particles and their production from ocean bubble bursting,
1398 Proceedings of the National Academy of Sciences, 107, 6652 - 6657, 2010.

1399 Russell, P. B., Livingston, J. M., Redemann, J., Schmid, B., Ramirez, S. A., Eilers, J., Kahn, R., Chu, D.
1400 A., et al.: Multi-grid-cell validation of satellite aerosol property retrievals in INTEX/ITCT/ICARTT
1401 2004, Journal of Geophysical Research - Atmosphere, 112, doi:10.1029/2006JD007606, 2007.

1402 Russell, P. B., Redemann, J., Schmid, B., Bergstrom, R. W., Livingston, J. M., McIntosh, D. M.,
1403 Ramirez, S. A., Hartley, S. A., et al.: Comparison of aerosol single scattering albedos derived by diverse
1404 techniques in two North Atlantic experiments, Journal of Atmospheric Science, 59, 609 - 619, 2002.

1405 Ryerson, T. B., Andrews, A. E., Angevine, W. M., Bates, T. S., Brock, C. A., Cairns, B., Cohen, R. C.,
1406 Cooper, O. R., et al.: The 2010 California Research at the Nexus of Air Quality and Climate Change
1407 (CalNex) field study, Journal of Geophysical Research - Atmospheres, 118, 10.1002/jgrd.50331, 2013.

1408 Savoie, D. L. and Prospero, J. M.: Water-soluble potassium, calcium, and magnesium in the aerosols
1409 over the tropical North Atlantic, Journal of Geophysical Research - Atmosphere, 85, 385 - 392, 1980.

1410 Schauer, J. J., Mader, B. T., DeMinter, J. T., Heidemann, G., Bae, M. S., Seinfeld, J. H., Flagan, R. C.,
1411 Cary, R. A., et al.: ACE-Asia intercomparison of a thermal-optical method for the determination of
1412 particle-phase organic and elemental carbon, Environmental Science and Technology, 37,
1413 10.1021/es020622f, 2003.

1414 Seinfeld, J. H.: Atmospheric chemistry and physics of air pollution, John Wiley1986.

1415 Shaw, G. E.: Sun Photometery, Bulliten of the American Meteorology Society, 64, 4 - 9, 1983.

1416 Smirnov, A., Holben, B. N., Slutsker, I., Giles, D. M., McClain, C. R., Eck, T. F., Sakerin, S. M.,
1417 Macke, A., et al.: Maritime aerosol network as a component Aerosol Robotic Network, Journal of
1418 Geophysical Research - Atmosphere, 114, doi: 10.1029/2008JD011257, 2009.

1419 Solarzano, L.: Determination of ammonia in natural waters by the phenolhypochorite method,
1420 Limnology and Oceanography, 14, 799 - 801, 1969.

1421 Stevens, B., Bondy, S., Farrell, D., Ament, F., Blyth, A., Fairall, C. W., Karstensen, F., Quinn, P. K., et
1422 al.: EUREC4A, Earth System Science Data, 13, 4067-4119, 2021.

1423 Swietlicki, E., Hannsson, H.-C., Hameri, K., Svenningsson, B., Massling, A., Mcfiggans, G., McMurry,
1424 P. H., Petaja, T., et al.: Hygroscopic properties of submicrometer atmospheric aerosol particles
1425 measured with H-TDMA instruments in various environments - A review, Tellus, 60B, 432 - 469, 2008.

1426 Turpin, B. J. and Lim, H.: Species contribution to PM2.5 concentrations: Revisiting common
1427 assumptions for estimating organic mass, Aerosol Science and Technology, 35, 602 - 610, 2001.

1428 Uno, I., Satake, S., Carmichael, G. R., Tang, Y., Wang, Z., Takemura, T., Sugimoto, N., Shimizu, A., et
1429 al.: Numerical study of Asian dust transport during the springtime of 2001 simulated with the CFORS
1430 model, Journal of Geophysical Research - Atmosphere, 109, doi: 10.1029/2003JD004222, 2004.

1431 Virkkula, A., Ahlquist, N. C., Covert, D. S., Arnott, W. P., Sheridan, P. J., Quinn, P. K., and Coffman,
1432 D. J.: Modification, Calibration and a Field Test of an Instrument for Measuring Light Absorption by
1433 Particles, Aerosol Science and Technology, 39, 68 - 83, 2005.

1434 Voss, K. J., Welton, E. J., Quinn, P. K., Johnson, J. E., Thompson, A. M., and Gordon, H. R.: Lidar
1435 measurements during Aerosols99, Journal of Geophysical Research - Atmosphere, 106,
1436 10.1029/2001JD900217, 2001.

1437 Wang, H. C. and John, W.: Particle density correction for the aerodynamic particle sizer, Aerosol
1438 Science and Technology, 6, 191 - 198, 1987.

1439 Wang, J., Christopher, S. A., Brechtel, F. J., Kim, J., Schmid, B., Redemann, J., Russell, P. B., Quinn,
1440 P. K., and Holben, B. N.: Geostationary satellite retrievals of aerosol optical thickness during ACE-
1441 Asia, Journal of Geophysical Research - Atmosphere, 108, 10.1029/2003JD003580, 2003.

1442 Wang, J., Flagan, R. C., Seinfeld, J. H., Jonsson, H. H., Collins, D. R., Russell, P. B., Schmid, B.,
1443 Redemann, J., et al.: Clear-column radiative closure during ACE-Asia: Comparison of multiwavelength

1444 extinction derived from particle size and composition with results from Sun photometry, Journal of
1445 Geophysical Research - Atmosphere, 107, https://doi.org/10.1029/2002JD002465, 2002.

1446 Weber, R. J., Orsini, D., Daun, Y., Lee, Y.-N., Klotz, P. J., and Brechtel, F. J.: A particle-into-liquid
1447 collector for rapid measurement of aerosol bulk chemical composition, Aerosol Science and
1448 Technology, 35, 718 - 727, 2001.

1449 Welton, E. J., Voss, K. J., Quinn, P. K., Flatau, P. J., Markovic, M. Z., Campbell, J. R., Spinhirne, J. D.,
1450 Gordon, H. R., and Johnson, J. E.: Measurements of aerosol vertical profiles and optical properties
1451 during INDOEX 1999 using micropulse lidars, Journal of Geophysical Research - Atmosphere, 107,
1452 10.1029/2000JD000038, 2002.

1453 Whittlestone, S. and Zahorowski, W.: Baseline radon detectors for shipboard use: Development and
1454 deployment in the First Aerosol Characterization Experiment (ACE 1), Journal of Geophysical
1455 Research - Atmosphere, 103, 16743 - 16751, 1998a.

1456 Whittlestone, S., Gras, J., and Siems, S. T.: Surface air mass origins during the First Aerosol
1457 Characterization Experiment (ACE-1), Journal of Geophysical Research - Atmosphere, 103, 16,341 -
1458 316,350, 1998b.

1459 Wiedensohler, A., Orsini, D., Covert, D. S., Coffman, D. J., Cantrell, W., Havlicek, M., Brechtel, F. J.,
1460 Russell, L. M., et al.: Intercomparison study of size dependent counting efficiency of 26 condensation
1461 particle counters, Aerosol Science and Technology, 27, 224 - 242, 1997.

1462 Witek, M., Flatau, P. J., Quinn, P. K., and Westphal, D. L.: Global sea-salt modeling: Results and
1463 validation against multicampaign shipboard measurements, Journal of Geophysical Research -
1464 Atmosphere, 112, doi:10.1029/2006JD007779, 2007.

Wood, R., Mechoso, C. R., Bretherton, C. S., Weller, R. A., Huebert, B. J., Straneo, F., Albrecht, B. A., Coe, H., et al.: The VAMOS Ocean-Cloud-Atmosphere-Land Study Regional Experiment (VOCALS-REx): goals, platforms, and field operations, Atmospheric Chemistry and Physics, 11, 627 - 654, 2011.

Yoneyama, K., Zhang, C., and Long, C. N.: Tracking pulses of the Madden-Julian Oscillation, Bulliten of the American Meteorological Society, 94, 1871 - 1891, 2013.

Young, J. F.: Humidity control in the laboratory using salt solutions, Journal of Applied Chemistry, 17, 241 - 245, 1967.

Zang, Z. and Liu, B. Y. H.: Performance of the TSI 3760 condensation nuclei counter at reduced pressures and flow rates, Aerosol Science and Technology, 15, 228 - 238, 1991.